AD NUMBER: AD0888844

LIMITATION CHANGES

TO:

Approved for public release. Distribution is unlimited.

FROM:

Distribution authorized to U.S. Government agencies only; Test and Evaluation; Jul 1971. Other requests shall be referred to Air Force Avionics Laboratory, Wright-Patterson AFB, OH 45433.

AUTHORITY

AFAL ltr dtd 29 Oct 1973

AFAL-TR-71-218

MEASUREMENT AND ANALYSIS OF MULTIPATH IN AIRCRAFT-SATELLITE COMMUNICATIONS LINKS AT UHF

John W. Mayhan

The Ohio State University
Research Foundation

FINAL TECHNICAL REPORT AFAL-TR-71-218
July 1971

Air Force Avionics Laboratory
Air Force Systems Command
Wright-Patterson Air Force Base, Ohio 45433

NOTICE

When Government drawings, specifications, or other data are used for any purpose other than in connection with a definitely related Government procurement operation, the United States Government thereby incurs no responsibility nor any obligation whatsoever; and the fact that the government may have formulated, furnished, or in any way supplied the said drawings, specifications, or other data, is not to be regarded by implication or otherwise as in any manner licensing the holder or any other person or corporation, or conveying any rights or permission to manufacture, use, or sell any patented invention that may in any way be related thereto.

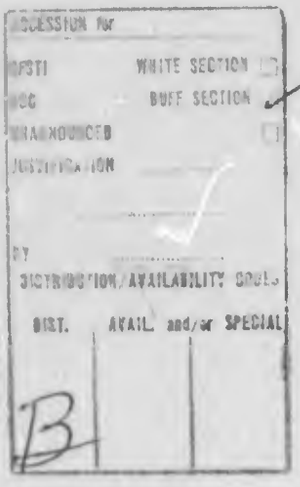

Copies of this report should not be returned unless return is required by security considerations, contractual obligations, or notice on a specific document.

AFAL-TR-71-218

MEASUREMENT AND ANALYSIS OF MULTIPATH IN AIRCRAFT-SATELLITE COMMUNICATIONS LINKS AT UHF

John W. Mayhan

FOREWORD

This report, AFAL-TR-71-218, OSURF Report Number 2734-1, describes the Measurement and Analysis of Multipath in Aircraft-Satellite Communications Links at UHF and was submitted by the author on 29 June 1971. This work was conducted during the period 1 November 1969 through 22 March 1971 by the ElectroScience Laboratory, Department of Electrical Engineering, The Ohio State University, Columbus, Ohio under Contract F33615-69-C-1089, Project No. 4164. Mr. L. L. Gutman, AFAL/AAI, was the Air Force Avionics Laboratory Program Monitor.

The report describes UHF up-link multipath data taken on 24-25 August 1970 with the airborne UHF transmitter terminal flying southeast of Goosebay, Labrador over water. Approximately 13 hours of data was acquired for satellite look angles from 0 to 12 degrees and an aircraft altitude of between 27,000 and 30,000 feet.

The multipath data acquisition, reduction, and analysis work was performed by the following OSU personnel: John W. Mayhan, William G. Swarner, Robert C. Taylor, and Judd D. Clover. Publication of this report does not constitute Air Force approval of the report's findings or conclusions. It is published only for the exchange and stimulation of ideas.

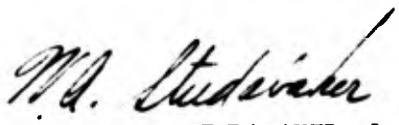

WILLIAM A. STUDABAKER, Lt Col, USAF
Chief, System Avionics Division
AF Avionics Laboratory

ABSTRACT

This final report summarizes the results of work performed during the period 1 November 1968 to 22 March 1971 under United States Air Force Contract F33615-69-C-1089. A major accomplishment of the work included measurements of multipath in an aircraft-satellite communication link at 300 MHz. Theoretical studies of aircraft-satellite communications links were also performed.

The experimental multipath tests were performed between an aircraft flying off the coast of Labrador and The Ohio State University Satellite Facility via the TACSAT satellite relay. Multipath returns were observed during various portions of the flight tests primarily while the aircraft was in a bank. Polaroid pictures and high speed motion picture data of the received signal were taken throughout the flight tests. The results of reducing 40 seconds of motion picture data (100 frames/second) indicated that the multipath return was essentially specular in nature (i.e., single ray multipath) with an amplitude 6 dB down from the direct signal. The polaroid photographs showed a range of multipath depths ranging from -4 to -9 dB.

TABLE OF CONTENTS

I. INTRODUCTION

The purpose of this report is to summarize the results of work performed under Contract F33615-69-C-1089 with the Air Force Avionics Laboratory, Wright-Patterson Air Force Base for the period of 1 November 1968 to 22 March 1971. The primary area of investigation was the measurement and analysis of multipath in an aircraft-satellite communication link at 300 MHz. Although the program emphasized experimental techniques, theoretical work was also performed to establish a base for the interpretation of results as well as to provide a better understanding of the phenomena governing the performance of aircraft-satellite communication links.

II. MEASUREMENT OF MULTIPATH IN AN AIRCRAFT-SATELLITE COMMUNICATION LINK AT 300 MHz

During the contract period, experimental tests were conducted to measure multipath in aircraft-satellite communication links at UHF. These tests were performed using an instrumented USAF/ASD C-135B jet aircraft S/N 61-2662, the TACSAT Satellite relay and a ground terminal provided and operated by ElectroScience Laboratory personnel of The Ohio State University. The aircraft-satellite-ground station geometry is shown in Fig. 1.

A simplified block diagram of the O.S.U. ground terminal system used to perform these tests is shown in Fig. 2. In this system, a thirty foot diameter antenna was used as an automatic tracking antenna (locked to the beacon signal of the satellite). A second thirty foot diameter antenna, which was used to receive the probing signal, was slaved to the tracking antenna. The received signal was appropriately amplified, translated to a 60 MHz I.F. frequency and demodulated by the Hazeltine modem.

The aircraft was equipped with three blade antennas, one dipole antenna and one crossed slot antenna mounted as shown in Fig. 3.

The experiment utilized a 6 Mb/s PSK, pseudo noise spread spectrum signal (i.e., a coded pulsed waveform). It was generated by the Hazeltine VIM-IA modem and was transmitted by the aircraft so that both the satellite (hence the direct path) and earth specular point (multipath) were included within the antenna beamwidth. The carrier frequency on the up link transmission (aircraft to satellite) was 300 MHz and 7.2 GHz on the down link transmission (satellite to O.S.U.). The spread spectrum signal was received at the O.S.U. ground terminal using a 53.5 dB gain (0.3^{o} beamwidth) antenna so that no additional multipath effects would be introduced to the

satellite to ground link. The received signal was then demodulated using the Hazeltine Vericode modem and single trace photographs of the correlator output were obtained from an oscilloscope display using an O.S.U. high speed (400 frames/sec maximum) motion picture camera synchronized with the received signal. The high speed motion picture film data was translated into digital form and onto magnetic tape by using the O.S.U. FOSDIC (Film Optical Scanning Device for Computer Input). The digital data, stored on magnetic tape, was then processed by means of appropriate computer algorithms. Polaroid photographs of the correlator output were also obtained. A description of the Hazeltine Vericode modem used in performing these experiments is provided in References 1 and 2.

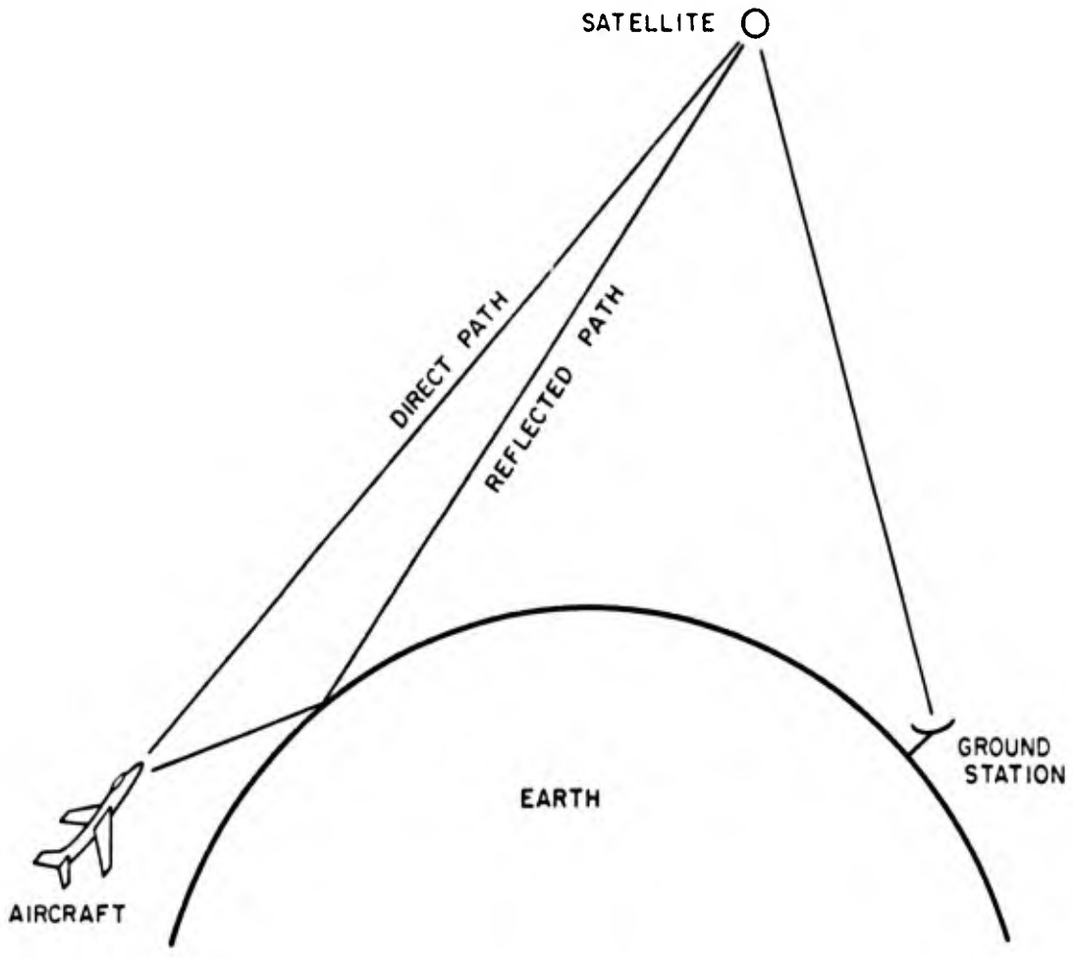

Fig. 1. Aircraft-satellite geometry.

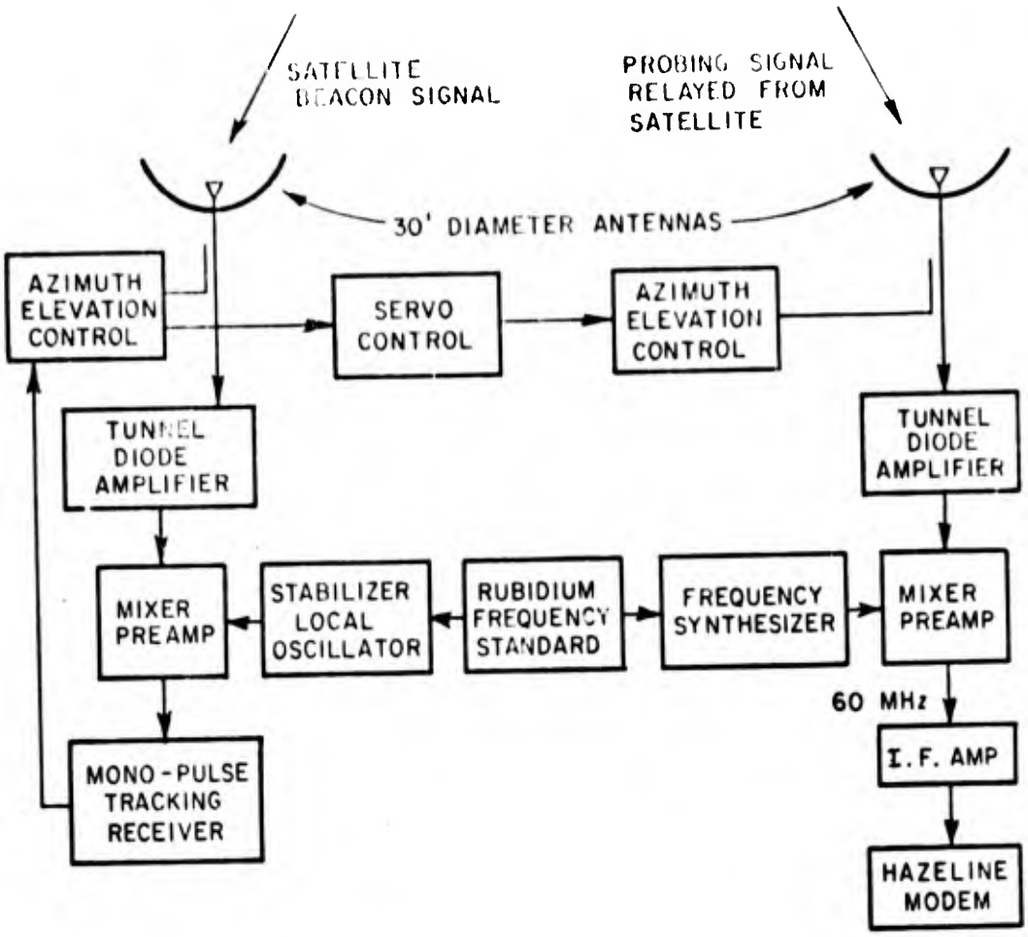

Fig. 2. Ground terminal system.

A. Test Results

Although there were various flight tests conducted the only successful ones were the flight tests conducted on the 24 and 25 of August, 1970, while the aircraft was in flight off the Coast of Labrador. At 15:00 z on the 24 of August 1970 the initial phase of the test series began. The signal from the Hazeltine VIM modulator was transmitted from the aircraft to O.S.U. via the TACSAT satellite relay during various periods of the scheduled flight plan. Although the direct signal was received at O.S.U. and classified as good, there were no observable multipath effects until approximately 18.40 z. At this time the aircraft was in a bank. Therefore, the remaining

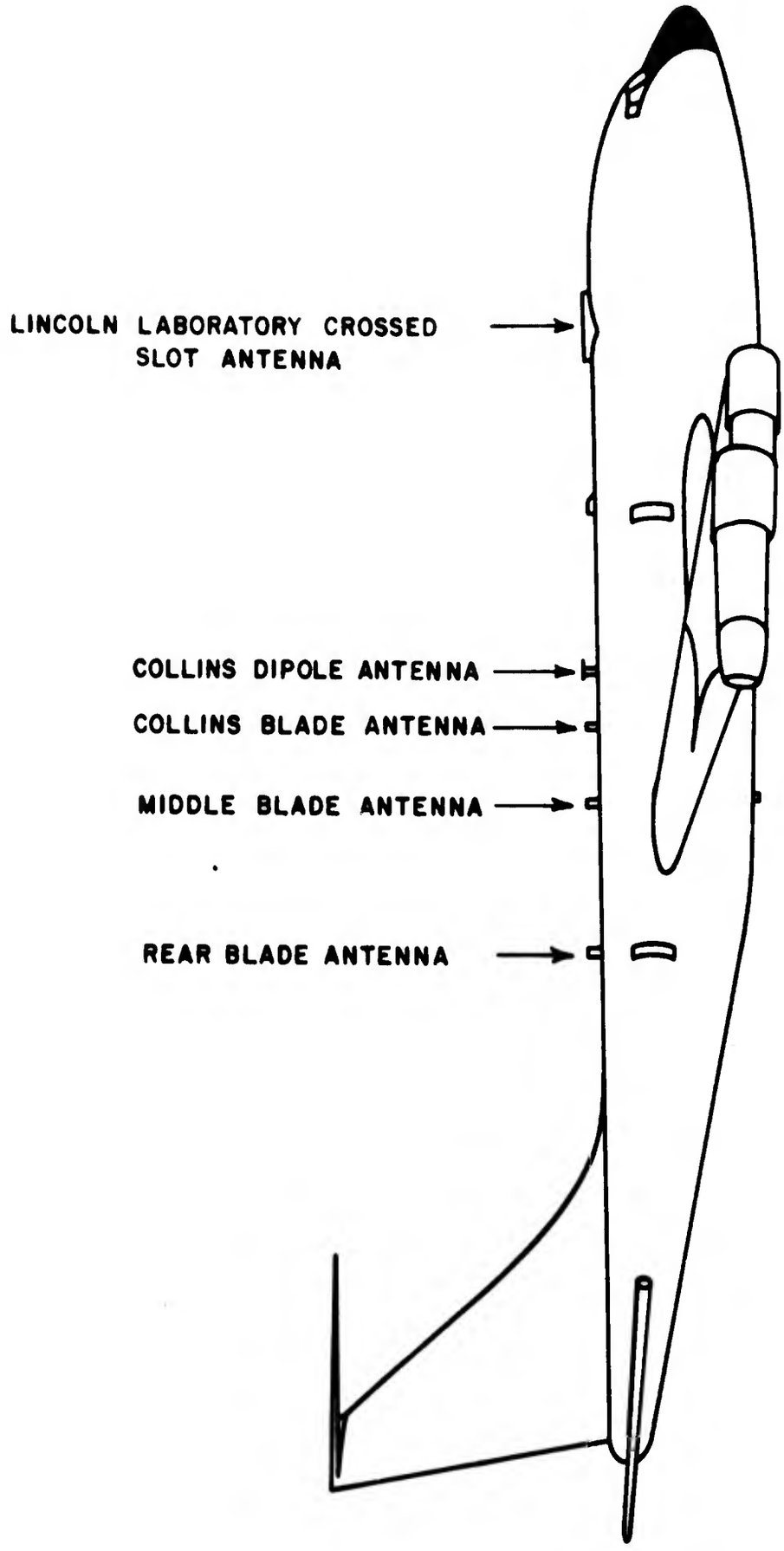

Fig. 3. UHF antennas on C-135 test aircraft.

flight scheduled for that day was modified to include more banks. Multipath effects were observed during each bank. Polaroid pictures and high speed motion picture data of the received signal were taken throughout the flight test.

At 10:00 z on August 25, the remaining portion of the test series was initiated. The first multipath effects were observed at approximately 10:37 z, again while the aircraft was in a bank. Further banks were performed by the aircraft throughout the remaining portion of the test and multipath effects consistently appeared during the banks. Furthermore, during the 13:00 z - 13:30 z flight plan, multipath effects were observed while the aircraft was flying in a straight line with a 4^{o} angle of attack. Polaroid pictures and high speed motion picture data of the received signal were taken throughout the flight tests.

Polaroid pictures of typical signals received at O.S.U. during the flight test are shown in Figs. 4 and 5. Most of these pictures were taken while the aircraft was in a bank. The first correlation pulse at the far left side of each photograph represents the correlation pulse due to the direct path. The second correlation pulse appearing in each photograph represents the correlation pulse due to the reflected path. The time delay between these respective pulses represent the difference between the time delay associated with the reflected path and the time delay associated with the direct path (i.e., differential time delay). The photographs of the received signals are presented in a sequence corresponding to the time of flight at which they were taken. The approximate elevation angle and bank angle of the aircraft corresponding to these times, as well as the differential time delay, are also labeled in the figure. The transmitting antenna corresponding to the data of Figs. 4 and 5 was the Collins blade. A photograph depicting single sweep motion picture data taken while the aircraft was flying in a straight line with a 4^{o} angle of attack is given in Fig. 6. The explanation of the polaroid picture data of Figs. 4 and 5 also applies to the motion picture data shown in Fig. 6.

B. Data Analysis

The high speed motion picture data taken during the flight test consisted of single trace recordings of good photographic quality suitable for scanning by the O.S.U. digital film reader. The examination of the film data showed that the multipath effects essentially consisted of a single sharp correlation pulse distinctly separated from that of the main correlation pulse. Spreading of the multipath signal (i.e., the appearance of either multiple peaks or a broad hump in the match filter output rather than a single sharp peak) was not evident by viewing the films.

The particular reel of film in which the maximum number of consecutive frames of obvious multipath appeared was chosen to start the data processing procedure. This reel of film corresponded to the case where the aircraft was flying in a straight line with elevation

Time ~ 10.55z
Elevation Angle ~ 3°
Differential Time
Delay ~ 3μ seconds
Bank Angle 30° Left

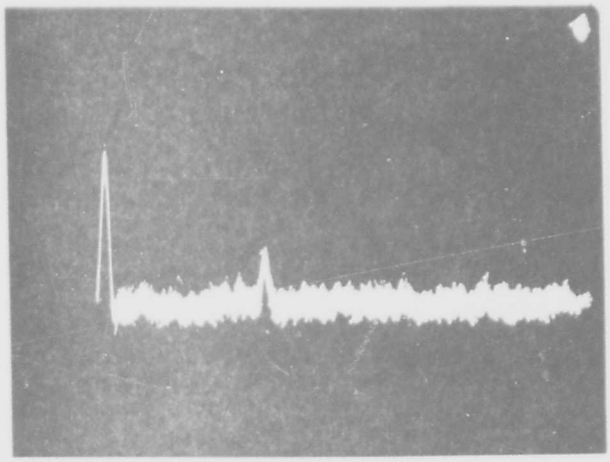

Time ~ 10.56z
Elevation Angle ~ 3°
Differential Time
Delay ~ 3μ seconds
Bank Angle 30° Left

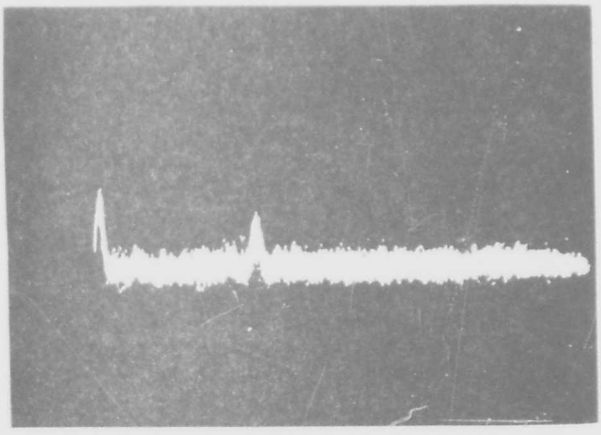

Time ~ 11.13z
Elevation Angle ~ 2°
Differential Time
Delay ~ 2μ seconds
Bank Angle 30° Left

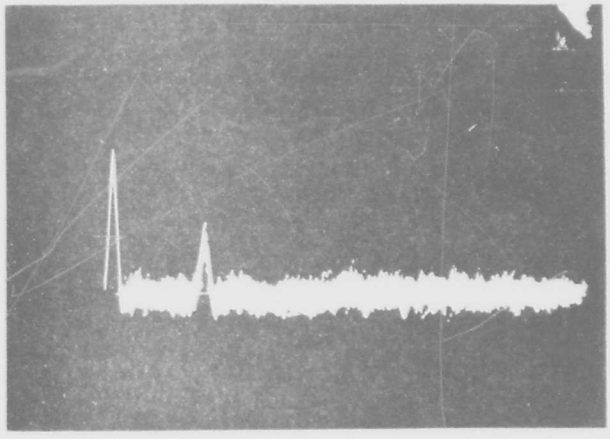

Fig. 4. Signal Received at OSU From an Aircraft Over the Atlantic Near Goose Bay Labrador. Antenna-Collins Blade. Date: 25 August 1970.

Time ~ 14.13z
Elevation Angle ~ 11°
Differential Time
Delay ~ 11μ seconds
Level Flight

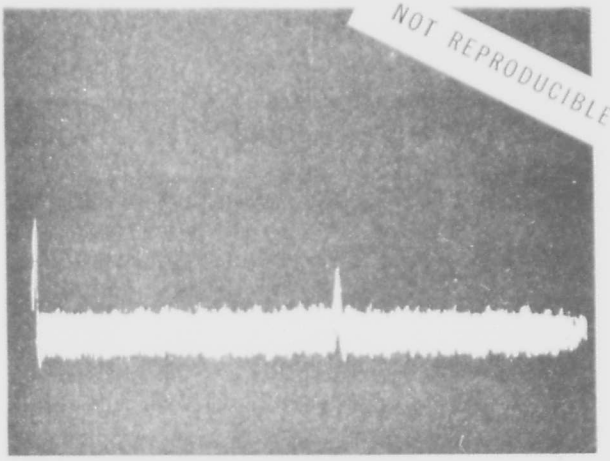

Time ~ 14.26z
Elevation Angle ~ 12°
Differential Time
Delay ~ 12μ seconds
Bank Angle 30° Right

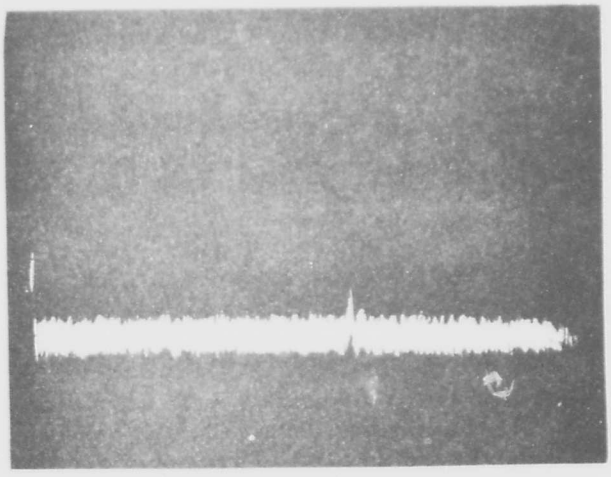

Time ~ 14.59z
Elevation Angle ~ 8°
Differential Time
Delay ~ 7.8μ seconds
Bank Angle 30° Right

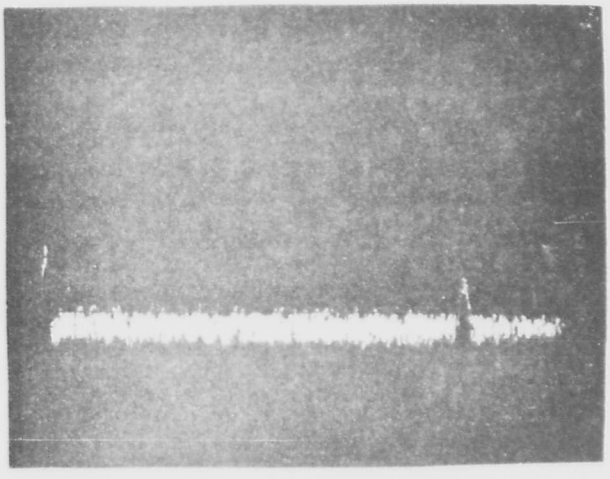

Fig. 5. Signal Received at OSU From an Aircraft Over the Atlantic Near Goose Bay Labrador. Antenna-Collins Blade. Date: 25 August 1970.

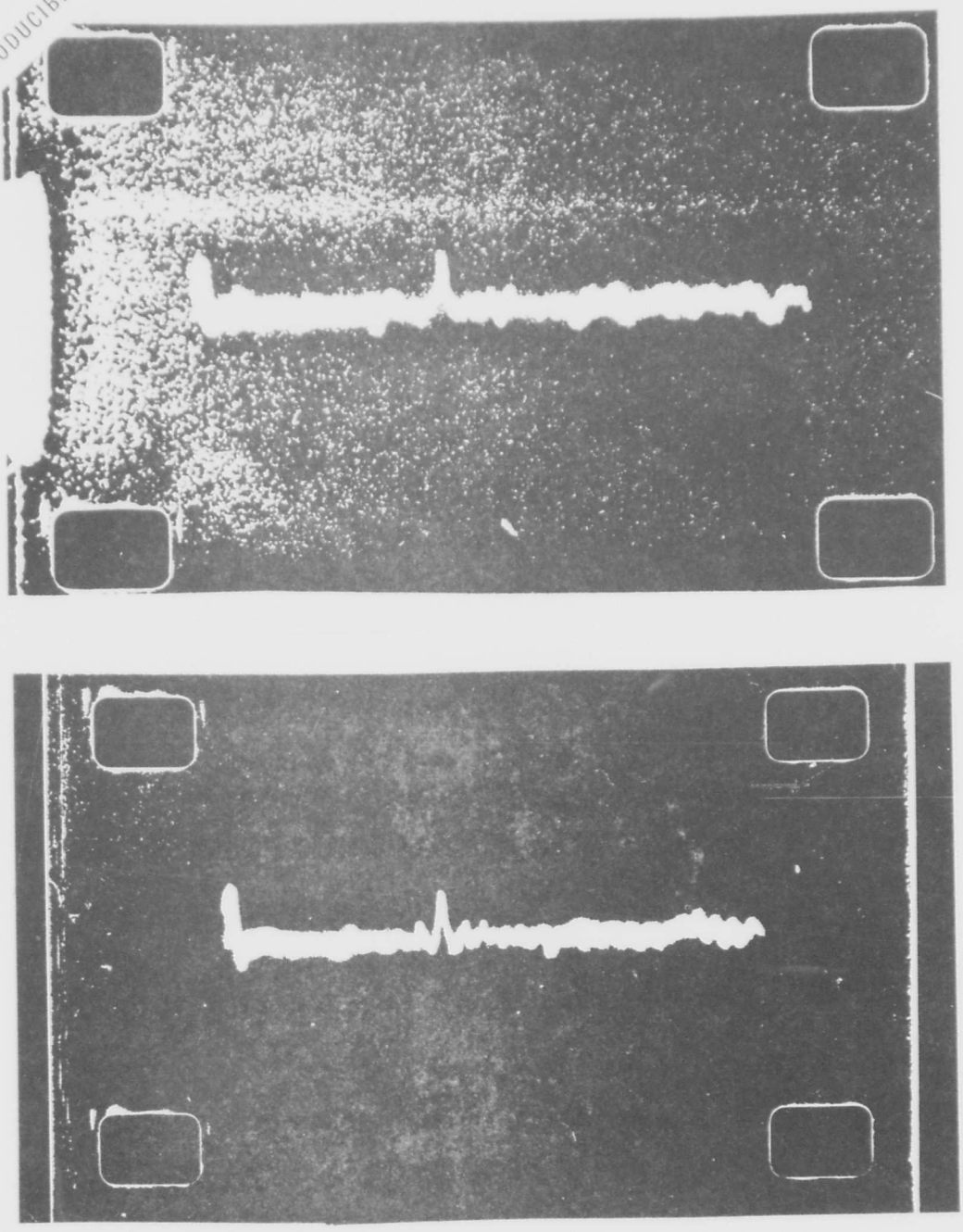

Fig. 6. Two Single frames of Multipath Returns Received at OSU from an Aircraft over the Atlantic Near Goose Bay Labrador. Antenna-Collins Blade. Time 13:18z. Date: 25 August 1970. Elevation Angle $\sim 5°$. Differential Time Delay $\sim 5\mu$ seconds.

angle, altitude and velocity of approximately 4 degrees, 30,000 feet and 400 miles/hour, respectively. The transmitting antenna corresponding to this data was the Collins blade. The motion picture data was scanned and digitized frame by frame using the O.S.U. digital film analyzer and the resulting digital data transferred to magnetic tape for further analysis. This transfer consisted of 4096 consecutive frames of motion picture data. The average speed of the camera at which these motion pictures were taken was 103 frames/sec. Thus the time sampling interval was approximately .01 seconds and the total duration of digitized data was approximately 40 seconds.

In order to calculate the differential time delay between the direct and multipath correlation pulses the entire waveform photographed (i.e., direct and multipath components) was digitized with a resolution of 7/64 μseconds. This resolution was sufficient for the accuracy desired in the calculation of the differential time delay. However, to accurately determine the peak amplitude of the direct and multipath components a greater resolution was required. In order to achieve this the direct and multipath components were digitized separately. The direct component was digitized with a resolution of 5/64 μseconds and the multipath component was digitized with a resolution of 1/16 μseconds. These latter two resolutions represent the maximum resolution that can be obtained for the direct and multipath components using the present capabilities of the O.S.U. scanner.

The first parameter calculated from the digitized data was the differential time delay between the direct and multipath components. For a single frame, this parameter is defined as the difference between the time of occurrence of the maximum of the multipath component and the time of occurrence of the maximum of the direct component. The calculated value of the differential time delay was found to be essentially constant over the entire data processing interval with a value of 3.9 μ second. This value agrees well with theoretical predictions of the differential time delay.

The next goal was to determine if any spreading of the multipath component had occurred. To achieve this an estimate of the time duration of the multipath component was obtained. In order to improve the accuracy of the time duration estimate frame by frame averaging was used. To explain this more precisely, reference is made to Fig. 7. Figure 7 depicts the motion picture frames of the multipath component arranged in a vertical sequence with the photographed signal of each frame digitized at values of τ corresponding to $\tau_j = j\Delta\tau$ ($j = 0, 1, \cdots 63$, $\Delta\tau = 1/16$ μsec). The variable τ represents the time coordinate on each frame. The sampled signal of the first frame is denoted by $m(0, j\Delta\tau)$, with the functional notation of zero denoting the first frame. Since the second frame corresponds to a time ΔT seconds later than the first frame ($\Delta T = 1/103$ seconds) the sampled signal of the second frame is denoted by $m(\Delta T, j\Delta\tau)$. This process is repeated until all the samples $m(n\Delta T, j\Delta\tau)$ ($n = 0 \cdots 4095$, $j = 0, \cdots 63$)

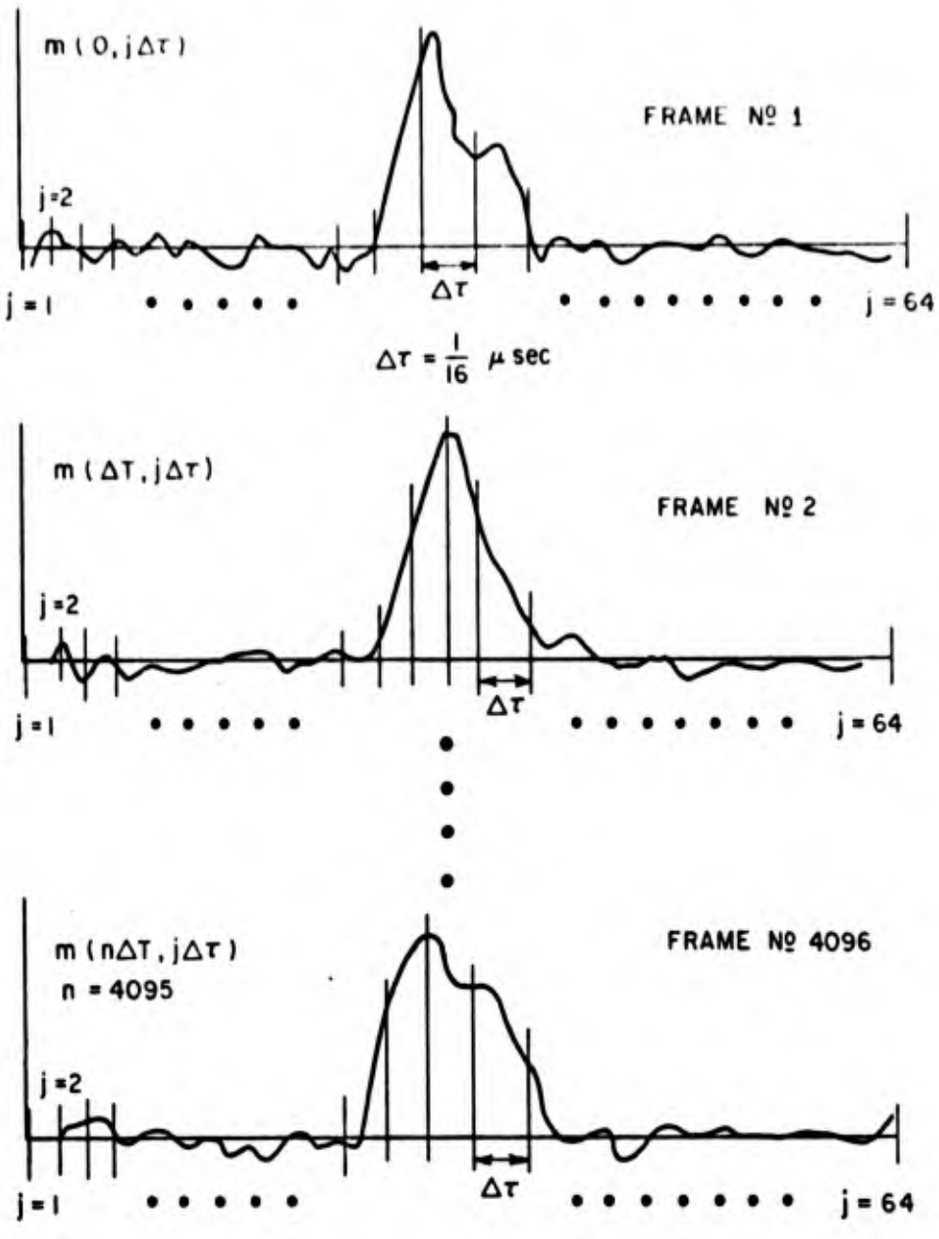

Fig. 7. Sampling process.

are obtained. For the subscript j fixed, the time sampled signal is denoted by $m_j(n\Delta T)$ and represents the time behavior of the jth sample of the photographed signal. The time average of this sampled signal, $\bar{m}_j$, is defined as

$$(1) \quad \bar{m}_j = \frac{1}{N} \sum_{n=0}^{N-1} m_j(n\Delta T).$$

Figure 8 depicts the values of $\bar{m}_j$ for values of j between 19 and 36 for N = 4096. The results of Fig. 8 show that there are at most five consecutive samples averages which may be considered to be above the average noise level of the system. These sample averages correspond to values of j between 25 through 29. The average noise level has an apparent nonzero value because of the position of the photographed signal on the digital scanner. It is concluded from the results of Fig. 8 that the time duration of the multipath component is essentially equal to the time duration of the correlation pulse width and therefore no multipath spreading was detected. Short time averaging was also performed using a value of N in Eq. (1) of 30. The results of these calculations also indicate that there are at most five consecutive sample averages which are above the mean noise level.

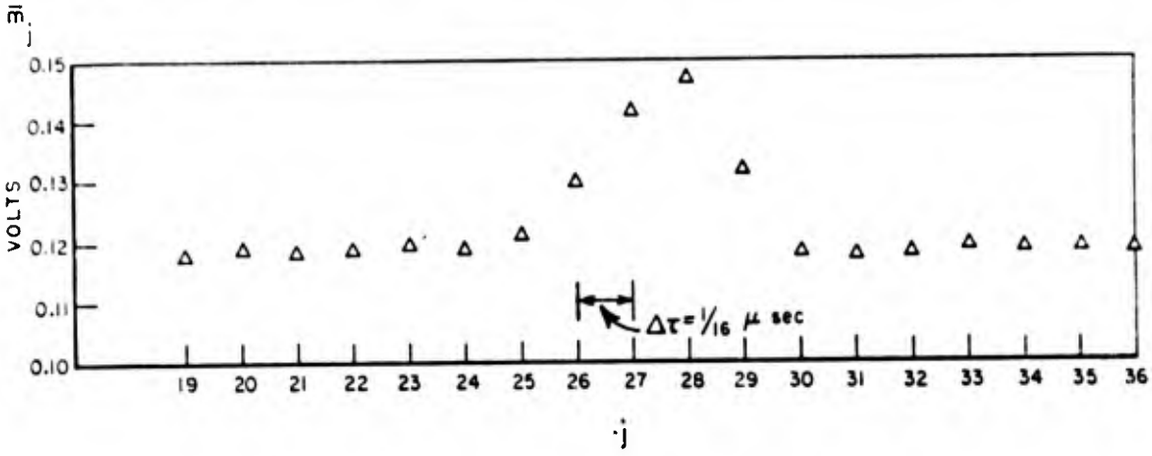

Fig. 8. Sample averages of the multipath component.

Estimates of the direct and multipath signal amplitudes were then obtained by determining the peak sample of each respective digitized signal. However, since the ratio of the resolution of the optical scanning device to the correlation pulse width is 15/64 for the direct component and 3/16 for the multipath component it was not certain that a reasonable estimate of the peaks had been obtained. Therefore, an alternate approach was taken in which the peak sample of the multipath signal along with two adjacent samples were jointly used to obtain an improved estimate of the peak by fitting these points to a parabola. An analogous procedure was also performed on the direct signal. Since the comparison of the peak sample to the improved estimate yielded

insignificant differences the actual peak value of each respective digitized component were used as an estimate of the direct and multipath signal amplitudes.

The fluctuation characteristics of a filtered version of the direct and multipath amplitudes were then analyzed by examining their frequency spectra and auto covariance properties. A filtered (averaged) version of a sampled signal is defined as that signal obtained by averaging over a given number of previous samples. Thus, if $g(n\Delta T)$ represents a sampled signal ($n = 0, \ldots N-1$) then a filtered version of $g(n\Delta T)$ using k-1 previous values is denoted by $g_k(n\Delta T)$ and is given by

$$(2) \qquad g_k(n\Delta T) = \frac{1}{k} \sum_{i=(n+1-k)}^{n} g(i\Delta T).$$

A filtered version of the signal is desirable in order to improve signal to noise ratio. The choice of k = 10 was used to obtain the filtered version of the direct and multiple amplitudes and corresponds to an averaging interval of 10 frames, or approximately 0.1 secs.

The square of the absolute value of the frequency spectrum (D.C. component removed) of the filtered version of the direct and multipath amplitude are shown in Fig. 9. These spectra were obtained by taking the absolute value of the discrete Fourier coefficients resulting from a fast Fourier transform of the filtered version of the direct and multipath amplitudes. It is evident from Fig. 9 that both the direct and multipath spectra have fluctuating components corresponding to the frequencies of 0.025 and 0.39 Hertz. Also labeled in Fig. 9 are the values of the D.C. components of the direct and multipath amplitudes.

In order to determine if there were any random components associated with the multipath amplitude fluctuations that could be attributed to rough surface scattering the time covariance function of the filtered version of the direct and multipath amplitudes were examined. The time auto covariance function of a time sampled signal $f(n\Delta T)(n=0\ldots N-1)$ is defined as $\psi_f(k\Delta T)$ ($k = 0 \ldots N-1$) and is given by

$$(3) \qquad \psi_f(k\Delta T) = \frac{1}{N-k} \sum_{n=0}^{N-1-k} f_R(n\Delta T)\, f_R(n\Delta T + k\Delta T)$$

where

$$(4) \qquad f_R(n\Delta T) = f(n\Delta T) - \frac{1}{N} \sum_{j=0}^{N-1} f(j\Delta T).$$

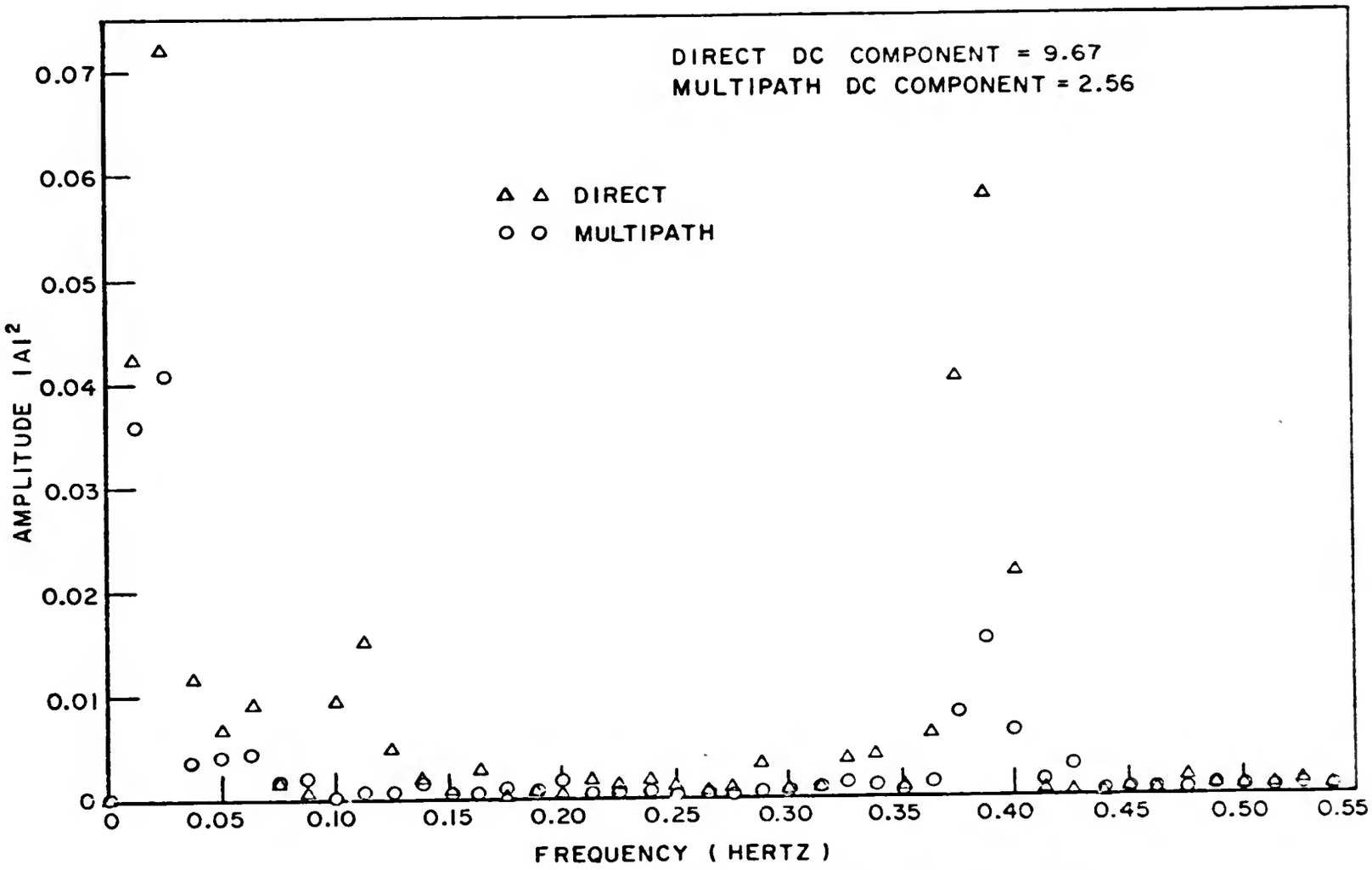

Fig. 9. Frequency spectra of direct and multipath amplitudes.

A portion of the sampled time auto covariance function of the filter version of the direct and multipath amplitudes are shown in Fig. 10 where a smooth curve has been drawn between the sample values. Both covariance functions are normalized to their values at $\tau = 0$. Figure 10 indicates that the direct and multipath covariance functions are very similar except for an amplitude factor. The periodic variations corresponding to the frequency of 0.39 Hertz (period $\sim$ 2.5 seconds) are clearly evident from the figure. The slow variation of the time covariance function i.e., the total nature of the curve, is due to the lower frequency components (0.025 Hertz, period $\sim$ 40 seconds) of the direct and multipath amplitudes. Only a portion of the total variation corresponding to this lower frequency component is evident from the covariance function since the total time displacement for which the covariance function is depicted is approximately one half of the period of the lower frequency component.

A final calculation was performed of the digitized data in order to provide an indication of the relative amplitudes of the direct and multipath signal. This was achieved by determining the ratio of the time average value of the multipath amplitude to the time average value of the direct amplitude. This ratio was determined to be approximately 1/2 or -6 dB in power.

During portions of the U.H.F. multipath test series a sinusoidal (c.w.) signal was also transmitted to the satellite and received at the Ohio State University Satellite Facility. This was in addition to the coded pulsed waveform processed through the Hazeltine modem. A portion of the recorded results depicting the amplitude variations of the received signal is shown in Fig. 11. These amplitude variations were present throughout the test flights. The estimated period of these amplitude fluctuations determined from Fig. 11 is approximately 2.7 seconds. This independent estimate of the period of the amplitude of the received signal returning a transmitted sinusoid agrees (within experimental error) with the estimate of the period of the variations of the direct and multipath amplitudes as determined from the digitized data.

C. Interpretation of Results

The first important result obtained from the experiment was the fact that a multipath component of considerable magnitude was detected. Furthermore, the results obtained from the data reduction indicated that there was no detectable time spreading associated with the multipath returns. From this result a model for the multipath channel at 300 MHz (valid over the bandwidth of the transmitted signal, i.e., approximately 6 MHz) may be postulated. The channel reproduces the transmitted signal except for a modification of its amplitude and phase. A complete characterization of the multipath channel therefore requires only a characterization of the amplitude and phase. Since the Hazeltine modem is not a coherent system it was impossible to measure the phase variations of the channel.

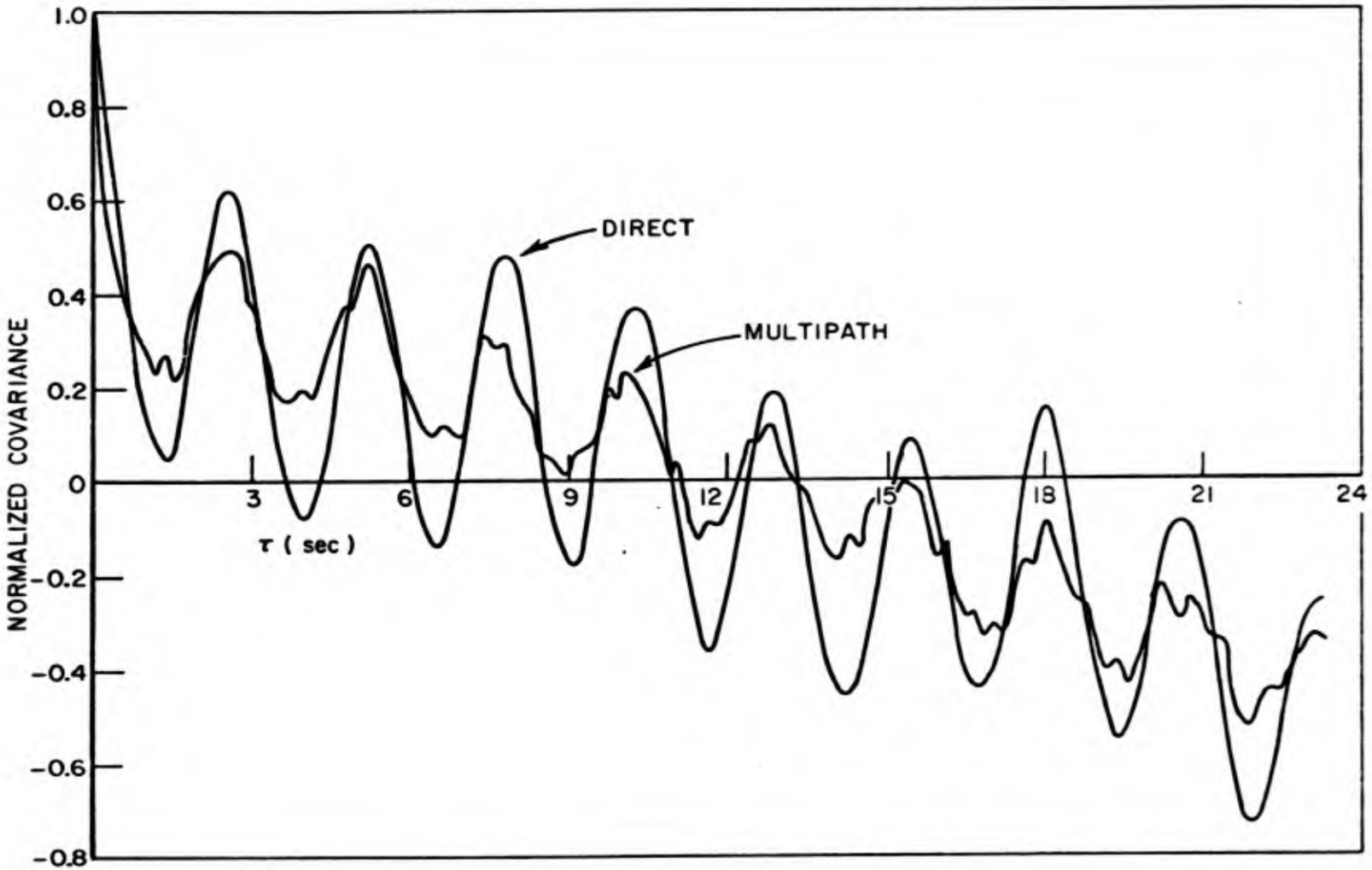

Fig. 10. Normalized time covariance function of direct and multipath amplitudes.

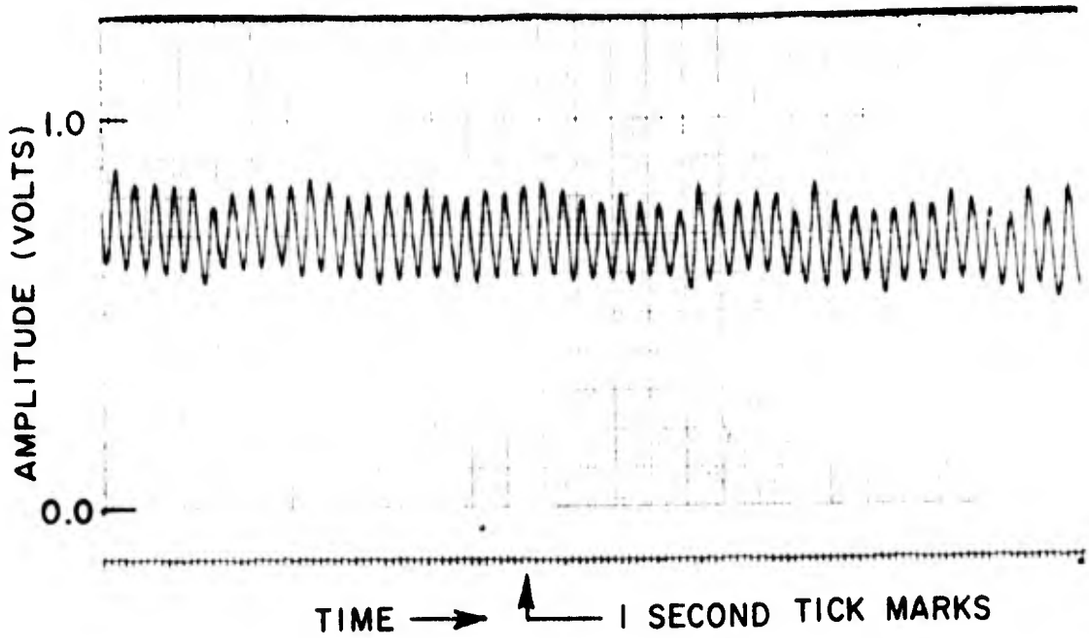

Fig. 11. Recording of the amplitude of the received cw signal.

The fluctuation characteristics of the direct and multipath signal amplitudes were analyzed by examining their frequency spectra and auto covariance properties. The results indicate that the direct and multipath signal variations are similar in nature and essentially consist of a periodic component with period approximately 2.5 seconds, and a much more slowly varying component of period approximately 40 seconds. Since the periodic component corresponding to the period of 2.5 seconds was also evident in the recordings of the amplitude of the received signal due to a transmitted sinusoid, it is concluded that satellite modulation (due to the motion of the satellite antenna) is the cause of these periodic variations. Furthermore, there is no evidence of any random components of appreciable magnitude in the multipath amplitude fluctuations that can be attributed to rough surface scattering.

The time variations corresponding to the lower frequency component observed in the direct and multipath amplitude spectra, however, did not appear on the strip chart recordings of the received signal due to a transmitted sinusoid. The precise nature of this slowly varying component cannot be fully characterized due to the duration of the processed data. It is possible, however, that this slow fluctuation of the amplitude is caused by variations in the processing gain of the modem.

Due to the above results, it is concluded that during the time interval corresponding to the processed data the scattering associated with the multipath channel at U.H.F., over the bandwidth of the transmitted signal, may be characterized as being essentially specular in nature.

The ratio of the amplitude factor associated with the multipath channel's transfer function and the amplitude factor associated with the direct channel's transfer function is -6 dB. Because of the uncertainties in the antenna pattern, this result has not been corrected for antenna gain. However, since the elevation angle of the aircraft during the time of flight corresponding to the processed data was small (approximately 4^{o}), this correction factor may be assumed negligible.

III. THEORETICAL CONSIDERATIONS OF MULTIPATH IN AIRCRAFT-SATELLITE COMMUNICATION LINKS

In order to provide a base against which experimentally determined results may be compared, as well as to provide a better understanding of the phenomena governing the performance of aircraft-satellite communications links, theoretical studies relating the physical parameters of an aircraft-satellite communication link to the measurable parameters were performed. The physical parameters of the communication link considered were 1) the directivity of aircraft and satellite antennas, 2) geometry (including motion) of aircraft and satellite and 3) the average reflection coefficient and radar cross section per unit area of the scattering surface associated with the multipath transmission. The average reflection coefficient and radar cross section per unit area in turn depend on the geometry (i.e., angle of incidence and reflection), frequency and polarization of the transmitted signal, and the electrical and statistical properties of the scattering surface.

Consideration was given only to the cases where the earth's surface associated with the multipath reflection may be modeled as 1) a perfectly smooth reflecting surface, and 2) a very rough reflecting surface. The experimentally measured parameters (i.e., the differential time delay and the ratio of the power received over the reflected path to the power received via the direct path) determined from the multipath tests described in the previous section are also compared with the theoretical results.

A. Smooth Earth Reflections

The important measurable parameters corresponding to the case of reflections from a smooth spherical earth are 1) the differential time delay, $\Delta\tau$, defined as the difference between the time delay associated with the reflected path and the time delay associated with the direct path 2) the differential doppler, $\Delta\nu$, defined as the difference between the carrier frequency received over the direct path and the carrier frequency received over the reflected path, and 3) the power ratio, ρ, defined as the ratio of the power received over the reflected path to the power received via the direct path. These parameters are more precisely defined with reference to Fig. 12 which shows the reflection geometry for a smooth spherical earth. The

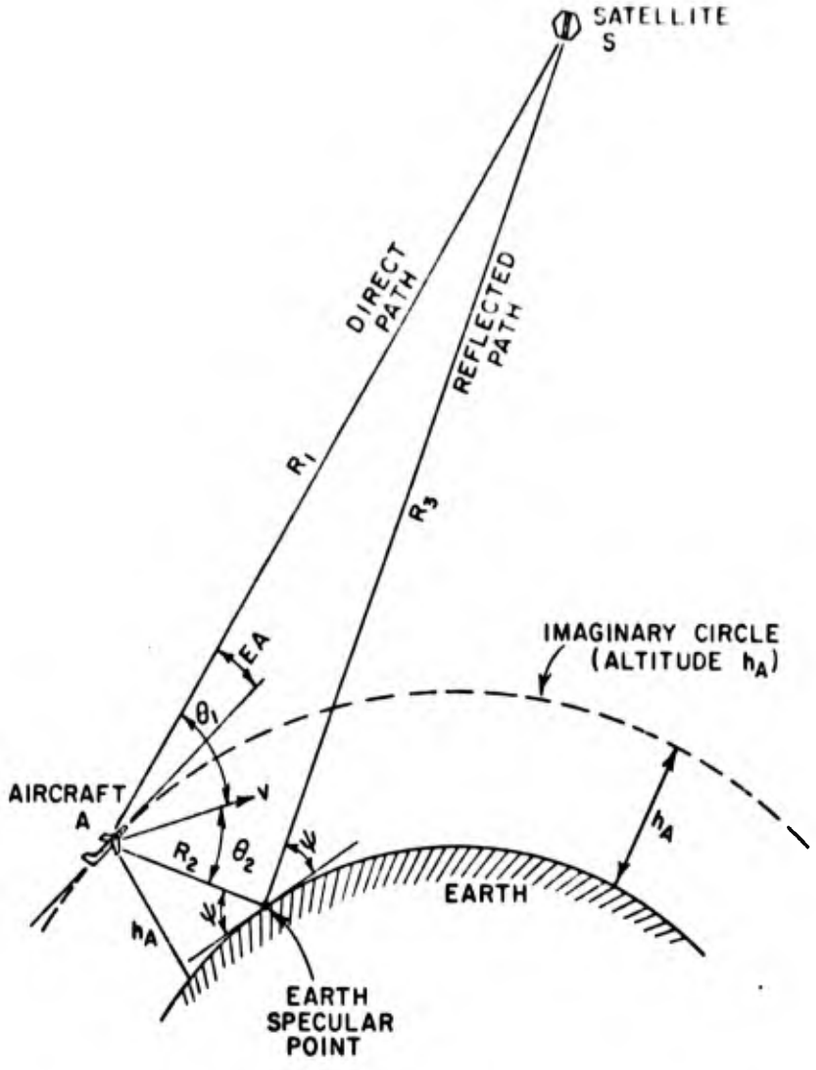

Fig. 12. Reflection geometry for a smooth spherical earth.

reflection geometry considered in Fig. 12 is specialized to the extent that the aircraft's velocity vector is assumed to lie in the plane containing the direct and reflected paths. Furthermore the satellite is assumed to be a synchronous satellite. Thus, no relative motion between the satellite and the earth is considered. In terms of the notation used in Fig. 12 the differential time delay is $\Delta\tau = (R_2 + R_3 - R_1)/C$, where C denotes the velocity of light and R_1, R_2 and R_3 denote the distance from aircraft to satellite, aircraft to earth's specular point, and earth's specular point to the satellite respectively. The differential doppler is $\Delta\nu = \omega_0 V (\cos\theta_1 - \cos\theta_2)/C$ where ω_0 denotes the carrier frequency and V the magnitude of the velocity vector of the aircraft. The angle θ_1 represents the angle between the velocity vector of the aircraft and the direct path and the angle θ_2 represents the angle between the velocity vector and the line joining the aircraft and earth's specular point.

The ratio of the power received via the reflected path to the power received via the direct path depends on the electrical properties of the reflecting surface as well as upon the specific geometry. An expression for this parameter corresponding to the geometry of Fig. 12 is derived in Reference 3 and consist of the products of four factors as $\rho = |\Gamma|^2 D^2 A_p^2 d^2$ where Γ represents the Fresnel reflection coefficient for a smooth plane surface and depends on the frequency, polarization, grazing angle and the electrical properties of the reflecting surface (see p. 396, Reference 3, for detailed expressions). The factor D^2 represents the divergence factor (Reference 3, p. 404) which accounts for the scattering from a spherical rather than a plane surface. The parameter A_p^2 represents the effect of the antenna gains of the aircraft and satellite antennas and d^2 represents the extra attenuation due to the additional path length traversed by the reflected path relative to the direct path.

To obtain numerically the above three parameters for a fixed position and velocity of the aircraft requires the determination of the earth's specular point. With the earth's specular point determined all other variables, i.e., grazing angle, range, etc., required to calculate the above parameters may be obtained. As the aircraft moves, however, the specular point changes and the parameters become a function of the aircraft's position. Figure 13 shows the dependence of the differential time delay on the elevation angle of the aircraft with respect to the satellite (i.e., the angle EA of Fig. 12) for altitudes of the aircraft corresponding to 10, 20, and 30 thousand feet. The altitude of the satellite used to obtain these results corresponds to that of a synchronous satellite (19327 n.m.). Also shown in Fig. 13 is the differential time delays as determined from the experimental multipath tests described in Section II. The experimental point denoted by the cross mark represents the value of the differential time delay as determined from the digitized data. The remaining experimental points (circles) represent the differential time delay as estimated from the polaroid photographs that were taken during the test series. The experimental values agree well with the theoretical predictions based on the smooth earth model.

Figure 14 depicts the differential doppler for the corresponding altitudes of the aircraft used in Fig. 13. The transmitted carrier frequency and aircraft velocity used to determine Fig. 14 were 300 MHz and 400 miles/hour respectively. Furthermore, the velocity vector of the aircraft was assumed to be tangent to an imaginary circle concentric with a spherical earth (see Fig. 12). The radius of this imaginary circle is $a_e + h_A$, where a_e denotes the radius of the earth and h_A the altitude of the aircraft.

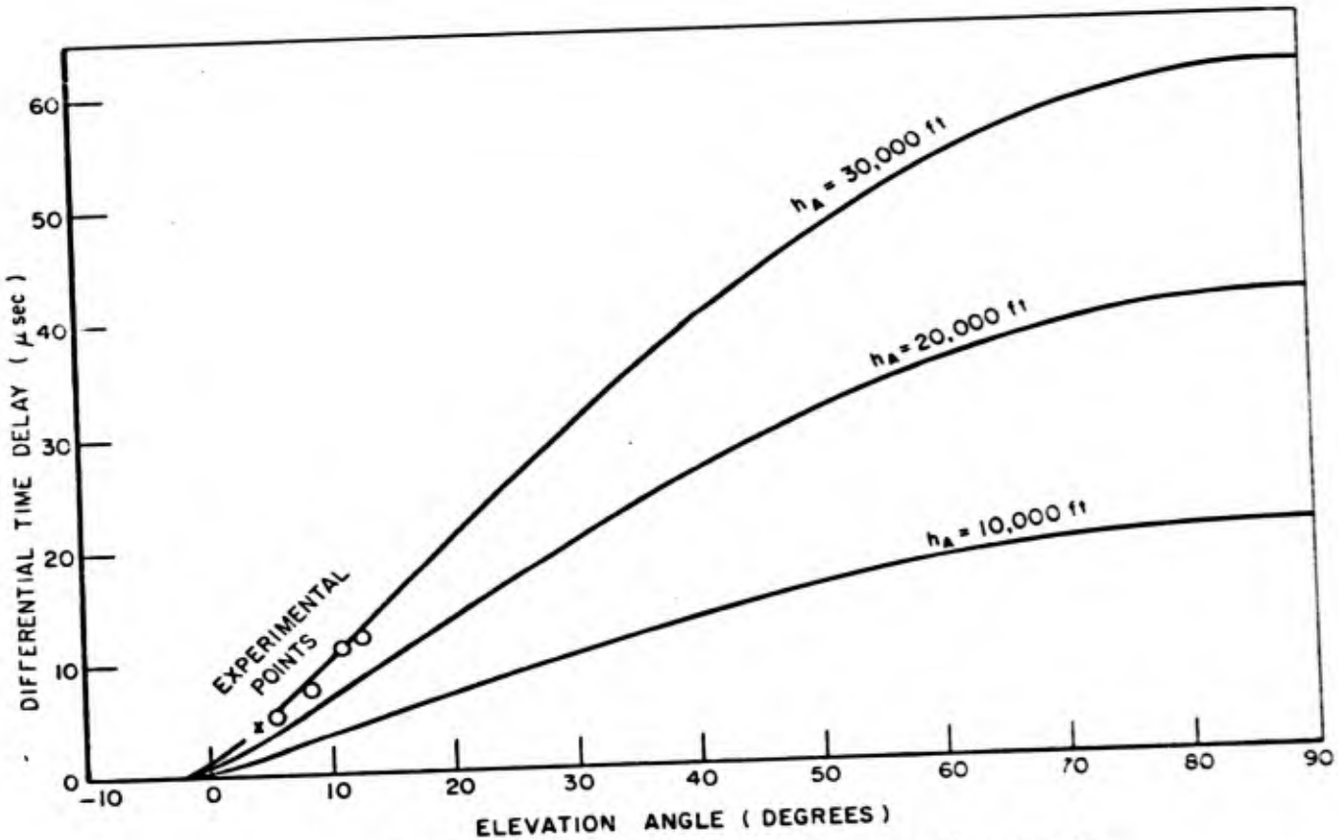

Fig. 13. Differential time delay vs elevation angle.

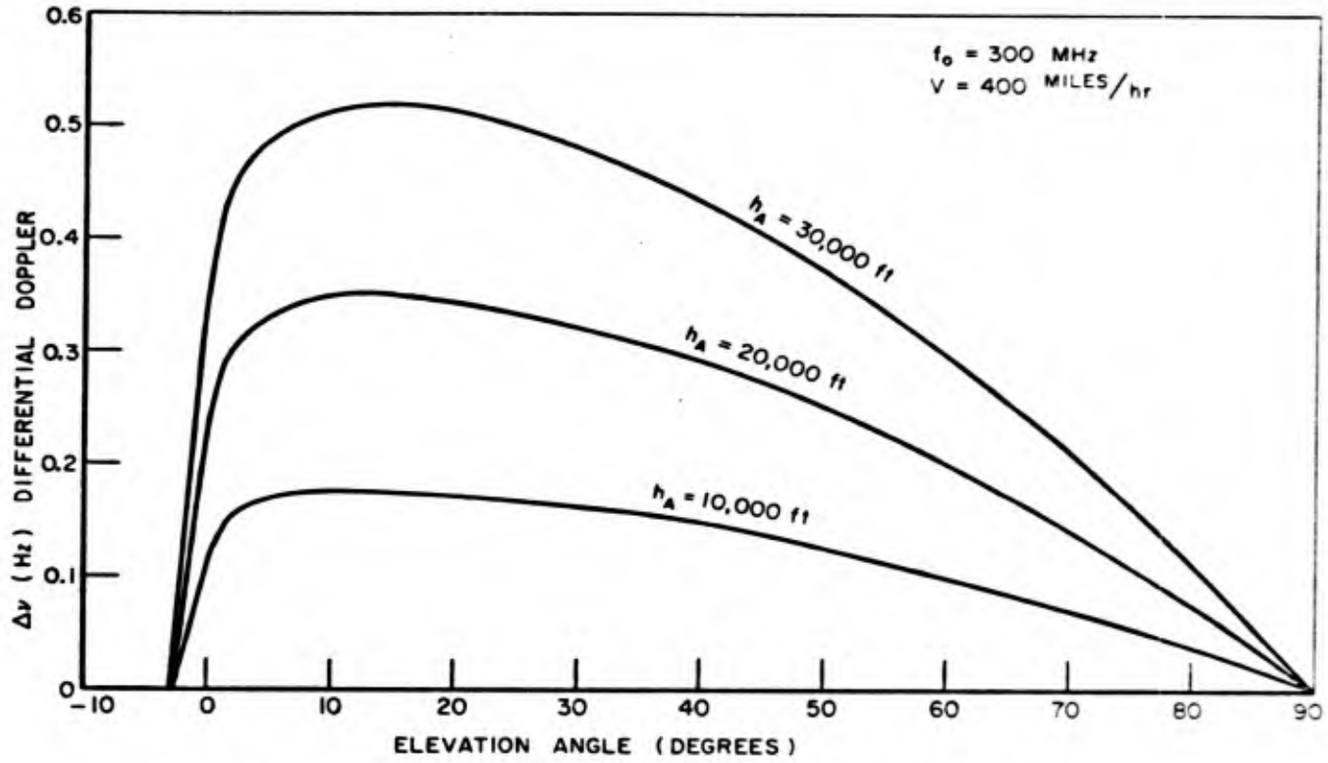

Fig. 14. Differential Doppler vs elevation angle.

The power ratio vs elevation angle of the aircraft for horizontal polarization, ρ_H^S, and vertical polarization, ρ_V^S, is shown in Fig. 15.

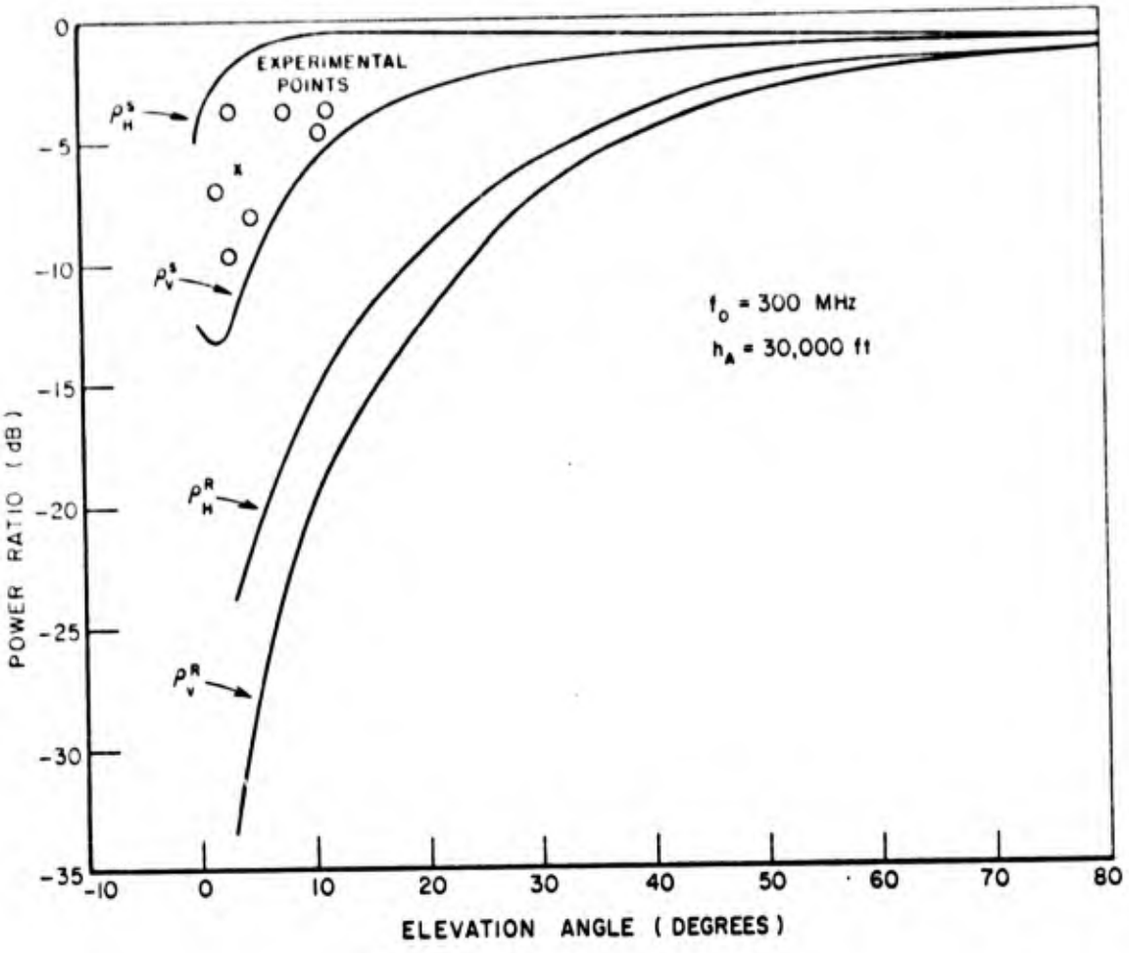

Fig. 15. Power ratio vs elevation angle.

The superscript S denotes the calculated value of the power ratio assuming a smooth surface model. Also shown in the figure are the power ratios of the direct and multipath signal amplitudes as determined from the previously described multipath tests. The curves labeled ρ_H^R and ρ_V^R of Fig. 15 denote the values of the power ratio corresponding to a rough surface model and will be explained in the next section. The curves corresponding to the power ratio of a smooth model of the reflecting surface were obtained by assuming an antenna parameter, A_p, of unity, a synchronous satellite, a carrier frequency of 300 MHz and an altitude of the aircraft of 30,000 feet. A relative dielectric constant of 80 and a conductivity of 4 mhos/meter were used in order to calculate the Fresnel reflection coefficient, Γ. These values are representative of an ocean surface.

The experimental point of Fig. 15 which is denoted by the cross mark represents the value of the power ratio as determined from the digitized data. The remaining experimental points (circles) represent the power ratios as estimated from the polaroid photographs that were taken during the test series. As is noted from Fig. 15 all the experimental points lie somewhere between the theoretical values predicted for a smooth surface assuming horizontal and vertical polarization. This result supports the conclusion that the multipath returns observed during the flight tests are primarily specular in nature.

A possible explanation for the fact that all of the experimental points fall between the horizontal and vertical polarization curves is that most of the multipath data was taken while the aircraft was in a bank. It is therefore possible that the polarization of the electric field incident on the reflecting surface was somewhere between vertical and horizontal polarization.

B. Rough Surface Reflections

The irregularities of the surface of the earth will introduce additional effects not contained in the smooth earth reflecting model. Two primary effects are the time and frequency spreading associated with the received signal. The gross transmission parameters characterizing these effects are the multipath spread, T_c, and the fading bandwidth, B_f. The multipath spread parameter is a measure of the maximum delay difference between the first and last significant propagation paths associated with the multipath reflections. It is completely determined by the relative geometries of the possible paths and by the relative velocity of propagation over the various paths. The fading bandwidth provides a measure of the bandwidth of the random component of the received waveform when the input to the multipath channel is a pure sinusoid. It is completely determined by the frequency of the sinusoid and by the relative motion of the various physical scatterers associated with the multipath transmission as well as the relative motion between the physical scatterers and the transmitting and receiving sites.

The power ratio corresponding to the case of reflections from a very rough surface (specular return absent) can be conveniently expressed in terms of the average radar cross section per unit area of the scattering surface associated with the multipath channel. In terms of the variables defined in the previous section, the power ratio ρR, is given by

$$\rho R = \int_A \rho_0 \, dA \tag{5}$$

where

$$(6) \qquad \rho_0 = \frac{1}{4\pi} D^2 \left[\frac{R_1^2}{R_2^2 R_3^2}\right] A_p^2 \sigma$$

and σ denotes the average radar cross section per unit area of the scattering surface. The integral of Eq. (5) is to be evaluated over the area defined by the intersection of the aircraft and satellite antenna patterns.

In order to numerically calculate the integral of Eq. (5) a model for the average radar cross section per unit area must be determined. The determination of the average radar cross section, given the electrical and statistical properties of the reflecting surface, has been the subject of considerable investigation in the literature.[4,5,6] The model chosen for σ is that derived by Beckman[6] and also utilized by Durrani[7] for similar calculations. It is given by

$$(7) \qquad \sigma = \frac{|\Gamma|^2}{2S^2 \cos^4 \gamma} \exp(-\tan^2 \gamma / 2S^2)$$

In Eq. (7), S is defined as the rms slope of the rough surface, Γ the Fresnel reflection coefficient of a smooth model of the surface, and γ is the angle mode by the bisector of the incident and reflected rays with the mean normal to the surface. Some of the more important assumptions on the derivation of Eq. (7) are 1) the surface height may be described by a Gaussian distribution about its mean level with an r.m.s. value of surface heights (i.e., the standard deviation) denoted by σ_0 and its correlation length denoted by T ($S \equiv \sqrt{2}\sigma_0/T$), 2) the physical optics approximation is valid with diffraction and multiple scattering neglected and 3) that σ_0/λ is "large" (λ is the wavelength of the incident radiation). For a more detailed discussion of the derivation of Eq. (7) Reference 6 should be consulted.

The calculated value of the power ratios for vertical and horizontal polarization corresponding to the above rough surface model are depicted in Fig. 15 for comparison with the specular values. In Fig. 15, ρ_V^R denotes the value of the power ratio for vertical polarization and ρ_H^R denotes the power ratio for horizontal polarization. The superscript R denotes calculation based on a rough surface model. The values of the rough surface power ratios depicted in Fig. 15 were obtained by using a value of σ_0/T of 1/40 and carrier frequency of 300 MHz. The altitude of the aircraft was 30,000 feet and the Fresnel reflection coefficient was obtained using the previous values of the relative dielectric constant and conductivity, i.e., 80 and 4 mhos/meter respectively. The antenna parameter A_p was again assumed unity. The results of Fig. 15 indicate that the corresponding power ratios of the rough surface model at large elevation angles are comparable to the values obtained from a smooth surface model. The large

ratios encountered at the high elevation angles (for both the smooth and rough surface models) however, can be reduced considerably by proper antenna design.

An approximation to the fading bandwidth and multipath spread as previously defined were also obtained using the model of the average radar cross section as defined in Eq. (7). In essence, these parameters were determined by locating the points on the earth surface where the integrand of Eq. (5) is down 10 dB from its maximum value. The resulting difference in doppler shifts, and the maximum time delay, were then used as an approximation to the fading bandwidth and multipath spread respectively. The results of these calculations are shown in Figs. 16 and 17. Figures 16 and 17 depict the fading bandwidth and multipath spread dependence on the elevation angle of the aircraft with σ_o/T as a parameter. The auxiliary parameters, i.e., velocity, altitude and carrier frequency used to determine these results are also indicated in the figures. As with the previous case involving doppler effects, the velocity vector of the aircraft was assumed tangent to an imaginary circle concentric with the earth. The radius of this imaginary circle is $a_e + h_A$ when a_e denotes the radius of the earth and h_A denotes the altitude of the aircraft.

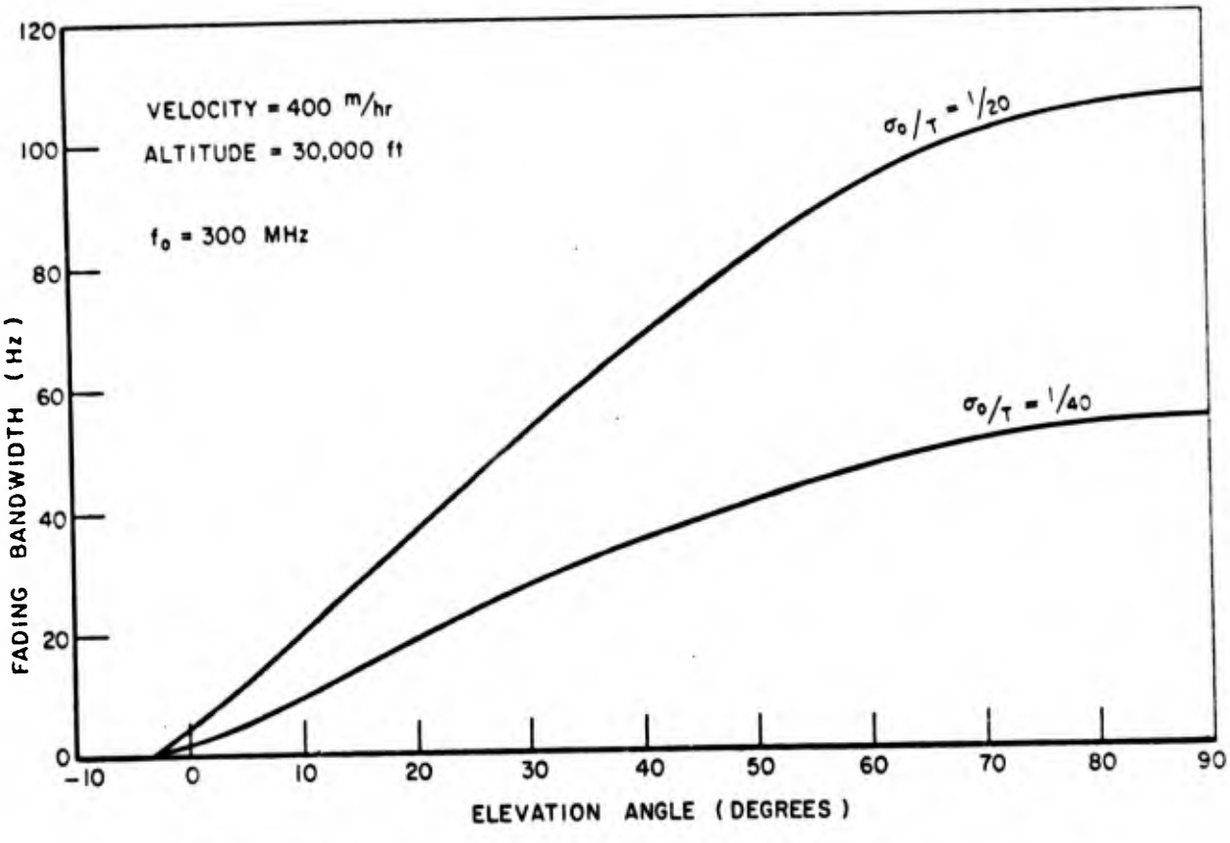

Fig. 16. Fading bandwidth vs elevation angle.

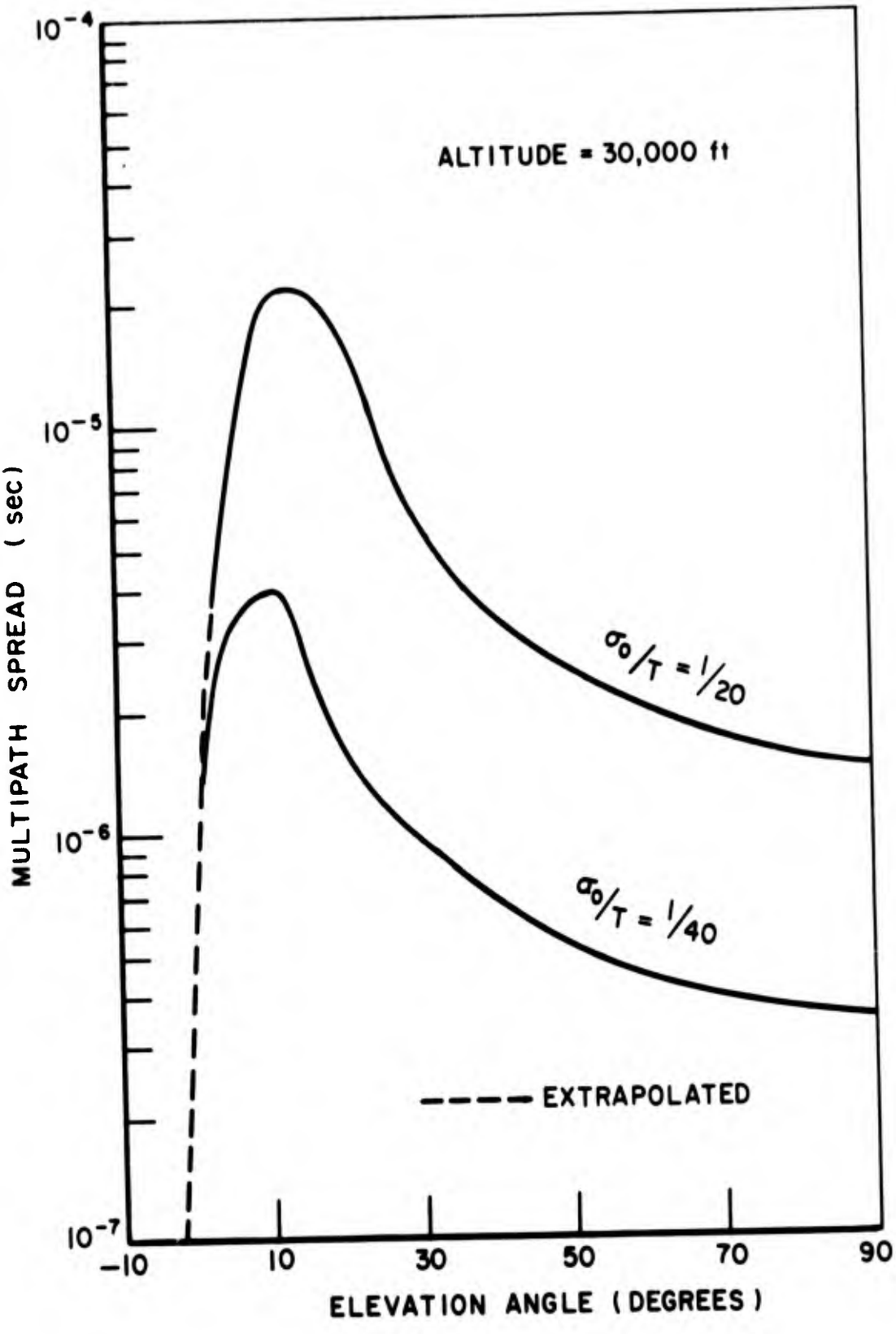

Fig. 17. Multipath spread vs elevation angle.

IV. PRELIMINARY INVESTIGATIONS OF EXPERIMENTAL TECHNIQUES FOR MULTIPATH CHANNEL CHARACTERIZATION

During the contract period an investigation was also performed to determine basic experimental techniques which are capable of achieving an adequate characterization of communications channels containing multipath transmission. These investigations put prime emphasis on the determination of modulation and demodulation techniques which are capable of measuring the impulse response function and transfer function of the transmission channel. Consideration was also given to the data processing required to obtain the mean values and covariance function of the experimentally determined impulse response function and the transfer function. These quantities are required to accurately evaluate the degradation in information transfer due to the transmission channel as well as to determine the modulation and demodulation techniques to combat adverse multipath effects.

The basic approach used to study transmission channels was the system function approach. In this approach the transmission channel is modeled by a randomly time variant linear filter. As is well known from the theory of linear system, the complete specification of a linear filter may be described by either its impulse response (time domain characterization) or by its transfer function (frequency domain characterization). Each of these system functions are defined as the characteristic response of the channel to a specific elementary excitation; namely, the impulse in time for the impulse response function and the impulse in frequency for the transfer function. When the filter is randomly time varying, however, the system functions become random processes and the channel is thus modeled by a randomly time varying system function. This approach is essential if a model of the communications channel is to be obtained which may be used with different waveforms. Therefore, before presenting the modulation and demodulation techniques which are theoretically capable of approximating the impulse response function, or transfer function, of the communications channel a brief discussion of the basic concepts underlying the system function approach will be given in the following section (Section A). This section also defines more precisely the mean value and covariance function of the transmission channel's system functions. Furthermore, the relationship between the gross transmission parameters characterizing the communication channel, i.e., the multipath spread, fading bandwidth, decorrelation time and coherence bandwidth, to the covariance function of the transmission channel's system function is presented.

A. Basic Description of the System Function Method of Channel Characterization

The system function method of characterizing communication channels has been used for some time (see Reference 8). In this approach one attempts to develop a general transfer relation between the transmitting and receiving terminals of a communications link. For this purpose it is convenient to use complex envelope notation. In this notation a narrow band transmitted signal $x(t)$ is represented as $x(t) = \text{Real}\{u(t)e^{i\omega_0 t}\}$ where the amplitude and phase of $u(t)$ represents the amplitude and phase modulations, and ω_0 denotes the carrier frequency. In the system function approach the channel is modeled as a linear time-variant filter. It therefore follows from the theory of linear systems that the output of the channel may be expressed as $y(t) = \text{Real}\{v(t)e^{i\omega_0 t}\}$ where

$$(8) \qquad v(t) = \frac{1}{2\pi}\int_{-\infty}^{\infty} T_{\omega_0}(t,\omega)\,\overline{U}(\omega)e^{i\omega t}\,d\omega$$

or equivalently as

$$(9) \qquad v(t) = \int_{-\infty}^{\infty} K_{\omega_0}(t,\tau)\,u(t-\tau)\,d\tau,$$

where $\overline{U}(\omega)$ denotes the Fourier transform of $u(t)$. In (8) and (9) $T_{\omega_0}(t,\omega)$ denotes the complex equivalent low pass transfer function of the channel and $K_{\omega_0}(t,\tau)$ denotes the complex equivalent low pass impulse response function of the channel, both referred to the carrier frequency ω_0.

Although the characterization of the channel via the system functions T_{ω_0} or K_{ω_0} may, in principle, be described, given the detailed knowledge of the mechanisms at work over the transmission medium, this approach is usually handicapped by the inability to predict these mechanisms in a deterministic sense. Therefore the system functions T_{ω_0} and K_{ω_0} are also modeled as random processes. Hence, a complete statistical characterization of the channel implies a knowledge of all probability distributions of the system function. It is usually impossible, however, to experimentally obtain this complete characterization. A more practical goal involves a second order statistical characterization in terms of mean values and covariance function of the system functions.

In general, the covariance function of K_{ω_0}, denoted by R_K and the covariance function of T_{ω_0}, denoted by R_T are expressed in terms of ensemble averages as

$$(10) \quad R_T(t_1,t_2;\omega_1,\omega_2)=\langle(T_{\omega_0}(t_1,\omega_1)-\langle T_{\omega_0}(t_1,\omega_1)\rangle)^*(T_{\omega_0}(t_2,\omega_2)-\langle T_{\omega_0}(t_2,\omega_2)\rangle)\rangle$$

$$(11) \quad R_K(t_1,t_2;\tau_1,\tau_2)=\langle(K_{\omega_0}(t_1,\tau_1)-\langle K_{\omega_0}(t_1,\tau_1)\rangle)^*(K_{\omega_0}(t_2,\tau_2)-\langle K_{\omega_0}(t_2,\tau_2)\rangle)\rangle$$

where * denotes the complex conjugate and $\langle\ \rangle$ denotes ensemble averages.

In many physical channels the random component of the system function may be assumed approximately stationary in the time variable so that the time-frequency covariance function, $R_T(t_1,t_2;\omega_1,\omega_2)$, and the cross covariance function of the impulse response, $R_K(t_1,t_2;\tau_1,\tau_2)$ depend only on the time difference $\Delta T = t_2 - t_1$. This assumption results in a wide sense stationary (w.s.s.) channel model.

One additional assumption is often made which allows a particularly simple characterization of the channel. This is the uncorrelated scattering (u.s.) assumption. Under the u.s. assumption the frequency dependence of the time-frequency covariance function depends only on the frequency difference $\Omega = \omega_2-\omega_1$. The w.s.s. assumption together with the u.s. assumption constitute a wide sense stationary uncorrelated scattering (w.s.s.u.s.) model of the channel. Under a w.s.s.u.s. channel model the time-frequency covariance function is denoted by $R_T(\Delta T,\Omega)$ and the cross covariance function of the impulse response reduces to

$$(12) \qquad R_K(\Delta T,\tau_1,\tau_2) = r_K(\Delta T,\tau_1)\ \delta(\tau_1-\tau_2).$$

In (12) $r_K(\Delta T,\tau)$ is defined as the channel autocovariance profile,[9,10] and $\delta(\tau)$ is the delta function. Admittedly, the uncorrelated scattering assumption is truly a nonphysical one since it assumes that the random components of the impulse response are uncorrelated for an arbitrarily small separation between sampling points. As will be discussed later, however, an approximation to the impulse response is obtained only at intervals comparable to the pulse width used in the probing signal. The actual assumption made, therefore, is that the random components of the impulse response are uncorrelated over sampling intervals separated by the duration of the pulse width, or greater. If this can be justified, then modeling the channel as an uncorrelated scattering channel will have no effect on the characterization of the channel over the bandwidth of the transmitted signal. The u.s. assumption will, of course, break down if one uses excessively wide band signals.

There are alternate representations of the covariance functions when the channel is a w.s.s.u.s. channel. The one most frequently used is that of the scattering function representation. The scattering function can be obtained by either a single Fourier transform of the auto covariance profile (with respect to ΔT) or by a two dimensional Fourier transform of the time-frequency covariance function. Other auxiliary or less inclusive, characterizations of the statistical properties of a w.s.s.u.s. channel are the delayed power density spectrum, frequency covariance function, doppler power density spectrum and time covariance function. In order to show the precise relations among these various descriptions reference is made to Fig. 18. In Fig. 18 the notation $S(\tau,\nu)$, $R_T(\Delta T,\Omega)$, $r_K(\Delta T,\tau)$ and $P_K(\nu,\Omega)$ denote the scattering function, time-frequency covariance function, auto covariance profile and doppler cross power spectral density and are four equivalent statistical characterizations of a w.s.s.u.s. channel. In Fig. 18 the notation $\leftrightarrow$ denotes a double

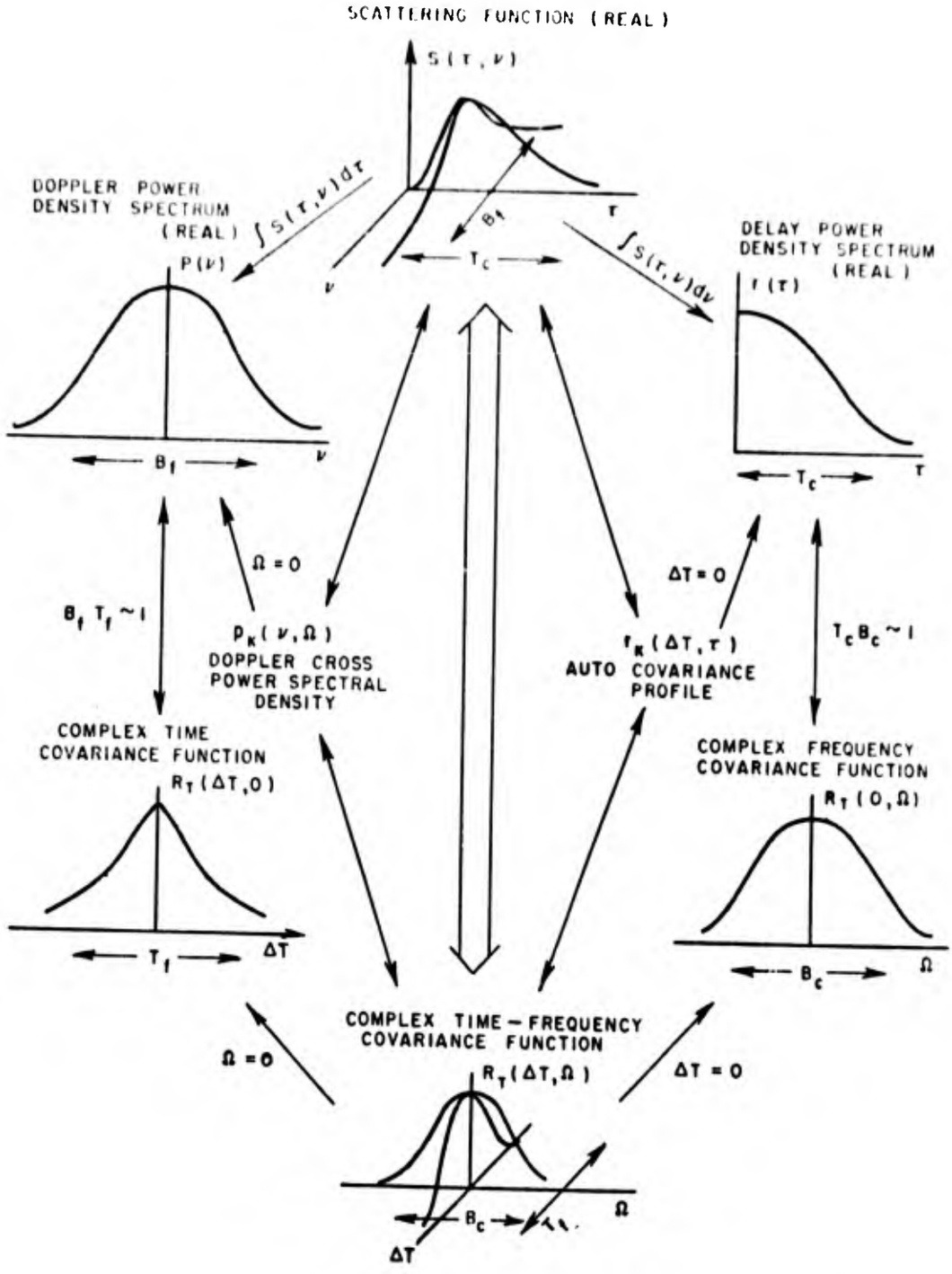

Fig. 18. The relationship between various statistical characterizations of a w.s.s.u.s. channel.

Fourier transform relation and ↔ a single Fourier transform relation. All quantities imply a carrier frequency ω_0. As will be discussed later, the use of a set of impulses in time essentially enables one to obtain $r_K(\Delta T,\tau)$, or the auto covariance profile, for discrete ΔT. The use of a set of sinusoids as a probing signal enables one to obtain the time-frequency correlation function for discrete Ω.

As shown in Fig. 18 a single Fourier transform (with respect to ΔT, ν being the inverse variable) of the auto covariance profile results in the scattering function $S(\tau,\nu)$. It can be shown that $S(\tau,\nu)$ is a real function. Physically, the scattering function represents the average power in the random component of the received signal at delay τ and doppler shift ν, when a unit sinusoidal tone is transmitted. The integral over all τ and ν gives the total power received.

The delay power density spectrum, $r(\tau)$, shown in the upper right hand side of Fig. 18 may be obtained by an integration of $S(\tau,\nu)$ over all ν or by evaluating the auto covariance profile at $\Delta T = 0$. Physically $r(\tau)$ represents the distribution of average power in the random component of the impulse response over the time delay τ. The frequency covariance function, shown in the lower right hand side of Fig. 18 is obtained by evaluating the time-frequency covariance function at $\Delta T = 0$, or by a Fourier transform of $r(\tau)$.

The doppler power density spectrum, $P(\nu)$, shown in the upper left hand side of Fig. 18 may be obtained by an integration of $S(\tau,\nu)$ over all τ or by evaluating the doppler cross power spectral density at $\Omega = 0$. Physically $P(\nu)$ represents the distribution of average power (over the doppler shift ν) in the random component of the received waveform when the input to the channel is a pure sinusoid. The time covariance function $R_T(\Delta T,0)$, shown in the bottom left hand side of Fig. 18, is obtained by evaluating the time-frequency covariance function at $\Omega = 0$, or by a Fourier transform of the doppler power density spectrum.

The gross transmission parameters characterizing the propagation medium (depicted in Fig. 18) are defined as the multipath spread, T_c, the fading bandwidth, B_f, the decorrelation time, T_f, and coherence bandwidth, B_c. The above parameters are not all independent. The multipath spread and coherence bandwidth are inversely proportional to each other as are the fading bandwidths and decorrelation time.

The multipath spread is defined as an appropriate width of either the scattering function over the variable τ or of an appropriate width of the delayed power density spectrum. Physically, this parameter is a measure of the duration of the random components of the impulse response. It is completely determined by the relative geometries of the possible paths and by the relative velocity of propagation over the various paths.

The fading bandwidth is defined as either an appropriate width of the scatter function over the ν axis or an appropriate width of the doppler power spectral density. It is a measure of the bandwidth of the random component of the received waveform when the input to the channel is a pure sinusoid. It is completely determined by the relative motion of the various physical scatterers associated with the channel as well as the relative motion between the physical scatterers and the transmitting and receiving sites.

B. Measurement Techniques

In the system function approach the second order statistical characterization of the channel is obtained via the mean values and covariance function of the system function. In order to obtain experimentally this characterization, however, one has to have available for suitable data processing a member of the respective system function. This section considers modulation and demodulation techniques which, in principle, can be used to obtain an approximation to the impulse response and transfer function of the communications channel.

1. Time domain measurement

The basic goal of the time domain measurement is to obtain an approximation to the impulse response function of the channel, $K_{\omega_0}(t,\tau)$. In words, $K_{\omega_0}(t,\tau)$ is described as; $K_{\omega_0}(t,\tau)$ = complex envelope of the channel response at time t, due to an impulse at carrier frequency, ω_0, applied at time $t-\tau$. Of course, an exact reproduction of the impulse response is physically impossible due to the unavailability of a true impulse. However a good approximation to the impulse response function, or more precisely a useable function of the impulse response function, may be obtained by probing the channel with extremely short pulses spaced periodically such that the response to one pulse does not overlap the response to the preceding pulse. More than one transmitted pulse is required in order to obtain the time variations of the channel. The response to a single pulse can be thought of as an approximation to $K_{\omega_0}(t_i,\tau)$ where t_i is the time of pulse transmission provided the channel does not change over the repetition period of the pulses.

To put the above idea on a more precise basis consider the system shown in Fig. 19. Figure 19 depicts the basic elements of a system that would be required to obtain a useable functional of the impulse response function using short pulses as a probing signal. In Fig. 19 the transmitted signal is assumed to consist of a periodic repetition (period T) of a narrow base band pulse, u(t), amplitude modulating a carrier signal at frequency ω_0. The received signal is processed at the front end of the receiver by a wide band amplifier. The output of the filter is then quadrature detected, filtered and recorded. Now let the quadrature outputs, labeled $\alpha(t)$ and $\beta(t)$ in Fig. 19, be expressed as a complex function of time $z(t) = \alpha(t) + i\beta(t)$. In the absence of additive noise the observed signal in the interval $nT < t < (n+1)T$ (i.e., between pulse transmission), may be then expressed as

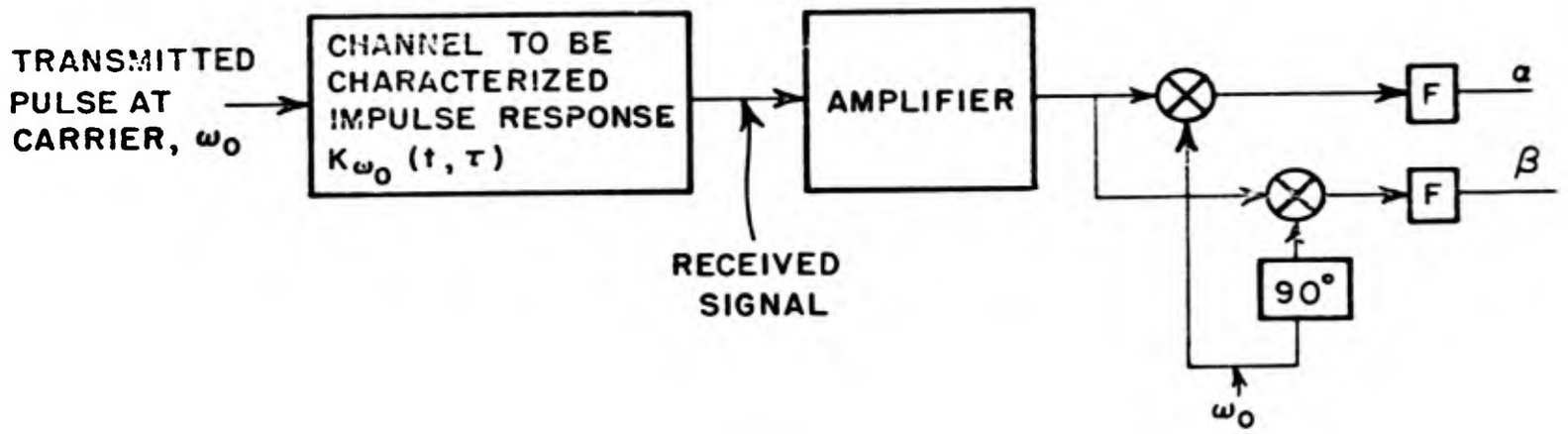

Fig. 19. Basic elements of a receiving system for short pulse transmission.

$$(13) \qquad z(nT,\iota) = \int_{\omega}^{\omega} K_{\omega_0}(nT,x)\, u(\iota-x)dx,$$

where $\iota (0 \leq \iota < T)$ is measured from the point $t = nT$ and represents the time scale between pulse transmissions. In the derivation of Eq. (13) it was assumed that the transmission medium does not change between successive pulse transmissions and also that the duration of the response of the channel to the transmitted pulse does not exceed the spacing between pulses.

Equation (13) represents the usable functional of the impulse response on which suitable data processing may be performed. In the ideal limit as $u(t)$ approaches the impulse function the observable output in the interval $nT < t \leq (n+1)T$ tends to $K_{\omega_0}(nT,\tau)$ directly.

In some applications, however, the use of a single narrow pulse has the principle disadvantage of requiring the generation of high peak power. This limitation can be overcome by transmitting an appropriately coded waveform of longer duration and using a filter matched to the transmitted signal at the receiving site. The basic elements of such a system is shown in Fig. 20. In Fig. 20 the transmitted signal is assumed to consist of a suitable code (i.e., a maximal length pseudo-noise (PN) sequence) phase modulating (0 or π) a carrier at frequency ω_0. Since a 0 or π phase modulation can be expressed as an equivalent ± 1 amplitude modulation, the transmitted signal is represented by $a(t) \cos \omega_0 t$ where $a(t)$ consists of the periodic repetition of the code (for the case shown in Fig. 20, also of period T). The received signal is processed at the front end of the receiver by a filter matched to $a(t)\cos \omega_0 t$. The output of the matched filter is then quadrature detected, filtered and recorded. As in the short pulse case, let the quadrature outputs labeled $\alpha(t)$ and $\beta(t)$ in Fig. 20 be expressed as a complex function of time $z(t) = \alpha(t) + i\beta(t)$. In the absence of additive noise the observed signal in the interval $nT < t < (n+1)T$ (i.e., between code transmissions), may be then expressed as

$$(14) \qquad z(nT,\tau) = \int_{-\infty}^{\infty} K_{\omega_0}(nT,x)\, R_{aa}(\tau-x)dx$$

where $\tau (0 \leq \tau < T)$ is measured from the point $t = nT$ and represents the delay interval between code transmissions. In Eq. (14) $R_{aa}(t)$ denotes the function composing the periodic correlation function of $a(t)$, i.e., $\phi_{aa}(t)$, defined in Fig. 20. In the derivation of Eq. (14) the previously used assumptions were again employed; that is, the transmission medium does not change during a code period and also that the duration of the response of the channel to the transmitted code does not exceed the code period.

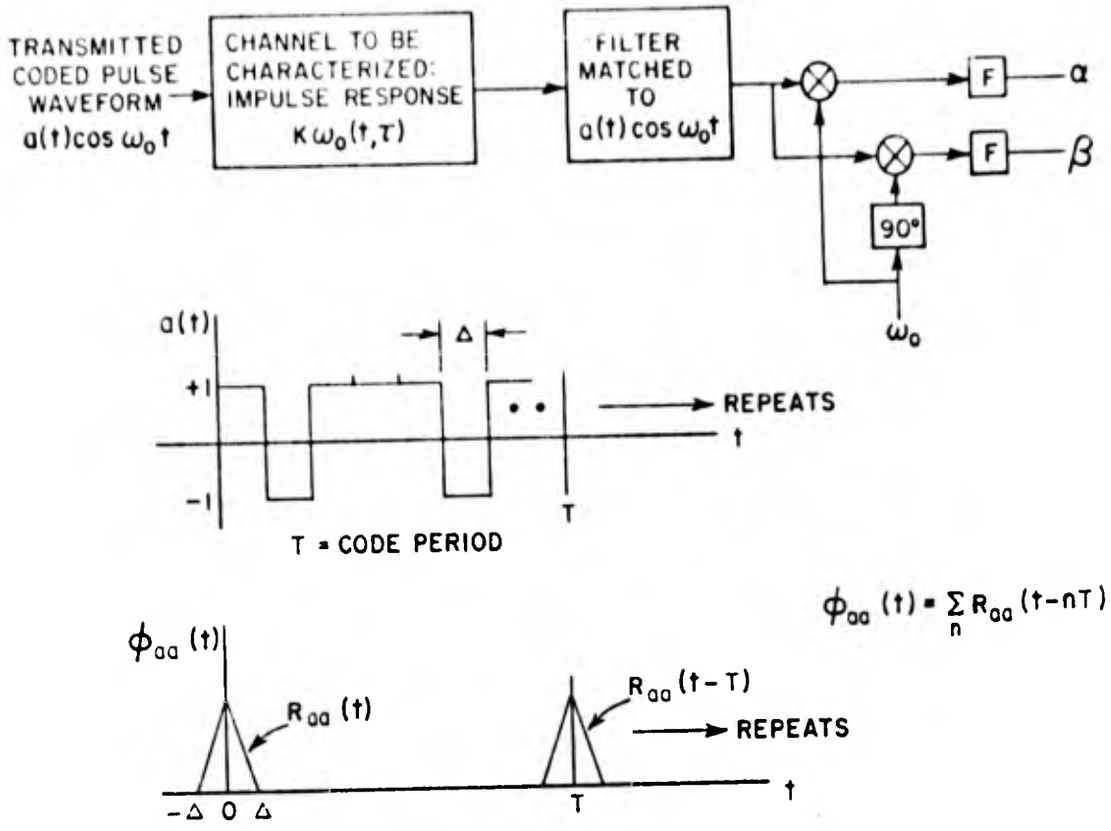

Fig. 20. Basic elements of the matched filter technique.

Equation (14) represents the useable functional of the impulse response for the matched filter case and is basically the same as Eq. (13) with the function $R_{aa}(t)$ replacing the transmitted pulse. In the ideal limit as $R_{aa}(t)$ approaches the impulse function the observable output tends to $K_{\omega_0}(nT,\tau)$ directly.

Theoretically, the measurement techniques just described require exact coherence between the transmitting and receiving sites in order to determine the complex impulse response of the channel. Exact coherence, of course, can never be achieved in practice. The effect of the differential phase instabilities between transmitting and receiving sites may be represented by a factor multiplying the received signal in its complex form (i.e., $z(t,\tau)$). This factor is given by $\exp[i\Delta\theta(t)]$, where $\Delta\theta(t)$ represents the differential phase between the reference oscillators employed at the transmitter and receiving sites. The consequence of the differential phase fluctuations is that they may become falsely interpreted as a phase variation of the channel which is being measured. When calculating power spectra of the received signal the multiplication of the output signal by the error term corresponds

to a convolution in the frequency domain by a spectral function whose bandwidth is inversely proportional to the differential phase fluctuations.

Usually, the differential phase variations may be modeled as $\Delta\theta(t) = \omega_d t + \phi(t)$ where ω_d denotes a frequency error (constant over the observation interval) defined so that the mean value of the random variations, $\phi(t)$, is zero over the observation interval. The effects of ω_d in the frequency convolution is to simply translate the spectrum while preserving its shape. This will manifest itself as an error in determining the mean frequency of the received signal. The random phase fluctuations, however, will limit the power spectral resolution that can be achieved.

In order to minimize the effect of the random component of the differential phase fluctuations crystal controlled frequency standards should be used at the transmitting and receiving sites. With the utilization of good reference sources the effect of the random component of the differential phase should be negligible. Furthermore, an estimate of the frequency offset, ω_d, could be made in order to compensate for its effect.

The data recording techniques used by O.S.U. in recent aircraft to satellite multipath experiments would also be applicable to the recording of the quadrature outputs from the time domain experiments. In this technique single trace photographs of the quadrature components would be obtained from an oscilloscope display (dual beam scope) using a high speed motion picture camera synchronized with the received signal. The high speed motion picture data would be analyzed by computer using the O.S.U. FOSDIC (Film Optical Scanning Device for Computer Input) for translating the photographic records into digital form and onto magnetic tape.

2. Frequency domain measurements

The goal of the frequency domain approach is to determine the time varying transfer function, $T_{\omega_0}(t,\Omega)$, defined as

$$(15)\quad T_{\omega_0}(t,\Omega) = [\text{response of the channel to } e^{i(\omega_0+\Omega)t}] \,/\, e^{i(\omega_0+\Omega)t}$$

The basic elements of a system which is capable of measuring $T_{\omega_0}(t,\Omega)$, for a fixed Ω, is depicted in Fig. 21. In Fig. 21 it is assumed that a c.w. signal of the form $\cos(\omega_0+\Omega)t$ is transmitted over the channel. It therefore follows from (15) that the received signal takes the form

$$(16)\quad |T_{\omega_0}(t,\Omega)| \cos [(\omega_0+\Omega)t + \theta_T(t,\Omega)]$$

where $\theta_T(t,\Omega)$ denotes the phase of the complex transfer function $T_{\omega_0}(t,\Omega)$. The received signal is then translated to an appropriate I.F. frequency quadrature detected and filtered as depicted in Fig. 21. The filtered outputs of the quadrature channels may then be shown to represent the real and imaginary parts of the complex transfer function $T_{\omega_0}(t,\Omega)$.

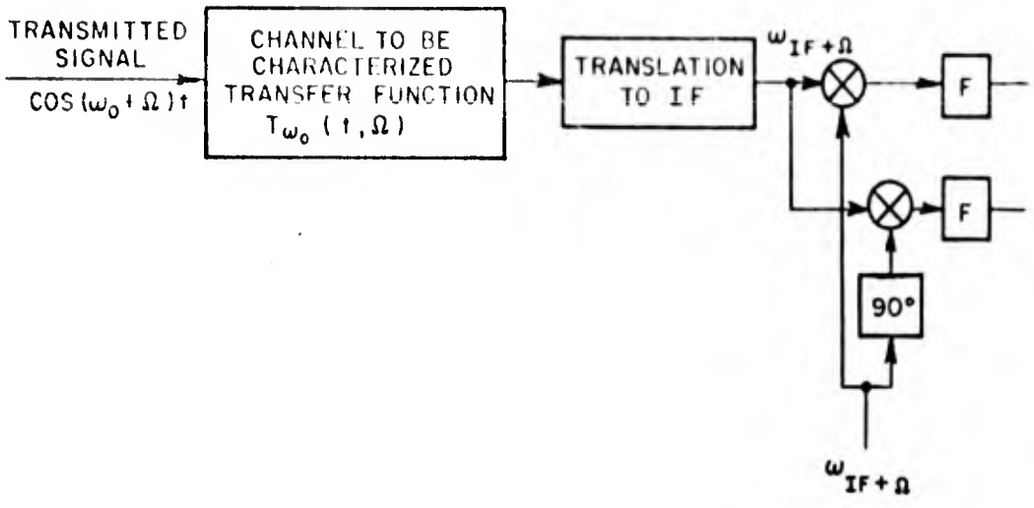

Fig. 21. Basic elements of a receiving system for a single frequency measurement.

This basic result leads quite naturally to a more complex system which simultaneously transmits a number of sinusoidal function as proposed by Bello[11]. In this system the transmitted signal is represented by a simultaneous transmission of N sinusoids having frequencies $\omega_0 + \Omega_i$ ($\Omega_i = i\Omega$, i = 1,N) where Ω represent the increments of the transmitted frequencies). The signal received at the front end of the receiver consist of a summation of a number of terms like that of Eq. (16). After hetrodyning to an appropriate I.F. frequency the individual received carriers are extracted by a bank of filters. In order that this may be achieved successfully in practice, however, the bandwidth of the individually received carriers must be significantly less than the increments of the transmitted frequencies. The output of each selective filter is then quadrature detected and filtered. The filtered output of each quadrature channel associated with the ith selective filter represents the real and imaginary parts of the complex transfer function $T_{\omega_0}(t,\Omega_i)$ (i=1,N) and are recorded on magnetic tape.

As discussed in the previously described time domain measurements, the frequency domain approach also requires the use of sufficiently stable frequency standards at the transmitting and receiving sites in order to obtain the complex transfer function of the transmission channel.

3. Data processing

The preceeding sections have described the basic elements and underlying principles of the modulation and demodulation techniques which have as their goal the attainment of a useable functional of the impulse response function of the channel, or the transfer function of the channel. In the time domain approach the observable output takes the form of a convolution integral involving the impulse response function, i.e., Eqs. (13) or (14), and in the frequency domain case the transfer function is recorded directly. The subject of the extraction of the mean values and covariance functions of the channel from the observed outputs will now be considered.

The data processing problem is not a trivial one and, in general, a solution cannot be obtained without making some physical assumptions about the nature of the observed process. The primary difficulty is that the desired quantities, i.e., the mean values and covariance function of the system functions are defined as ensemble averages. Unfortunately, in practice one does not have an ensemble of responses available, but only an observation of a single member of the process.

The first assumption required is that the random component of the observed output is such that ensemble averages can be obtained by time averages over various time intervals of the data. Although this assumption is reasonable, it deserves some comment since it is known that many physical channels do not exhibit statistical regularity over indefinitely long intervals of time. For example, many channels have been shown to exhibit a "fast" fading effect superimposed on slow (nonstationary) variations. In order to measure the covariance function of the fast variations of such a channel by time averaging, the data processing interval must be much less than the correlation time of the slow variations. However, in order to keep the measurement errors due to a finite sample length small, the data processing interval must be much greater than the correlation time of the "fast" fluctuations. Fortunately, many channels seem to satisfy these constraints and therefore it does not seem unreasonable to assume that time averaging may be performed over various intervals of the data. In general, however, the precise length of the data processing interval, as well as the actual justification of stationarity, is difficult to give prior to any specific experiment. Furthermore, the shortness of the interval over which stationarity may be assumed places a restriction on the frequency resolution that can be obtained.

To be more specific in the discussion, consider the case of the short pulse experiment. Due to the similarity of the recorded outputs of the short pulse technique and the matched filter approach, i.e., Eqs. (13) and (14), similar comments apply to the matched filter case.

Under the assumption of stationarity the cross covariance function of the random component of the recorded output of the short pulse technique, denoted by $C_Z(\Delta T,\tau_i,\tau_j)$, may be obtained by time averaging. In particular for each delayed sample values, τ_i and τ_j

$$(17) \qquad C_Z(\Delta T,\tau_i,\tau_j) = \langle Z_R(t,\tau_i)^* \, Z_R(t+\Delta T,\tau_j)\rangle_t$$

where the subscript t denotes time averaging and $Z_R(t,\tau_i)$ represents the random component of the recorded output. In the short pulse technique the observed output is related to the impulse response function of the channel by an integral equation of the convolution type. It therefore follows that the cross covariance of the random components of the observable output is related to the cross covariance of the impulse response, i.e., $R_K(\Delta T,\tau_i\tau_j)$ of Section IVA, by a double integral equation. If it can be shown that $C_Z(\Delta T,\tau_i,\tau_j) = 0$ for τ_i and τ_j separated by the duration of the probing signal, then the uncorrelated scattering assumption can be made. For this case the autocovariance profile completely specifies the covariance function of the impulse response and is related to the autocovariance function of the observable output, i.e., $C_Z(\Delta T,\tau_i\tau_i)$, by a single integral equation. Furthermore, for the case where the auto covariance profile, $r_K(\Delta T,\tau)$, has a duration (with respect to the τ variable) which is much greater than the duration of the probing signal, the auto covariance function of the random component of the observed output for values of τ separated by the duration of the probing signal may be directly used to approximate the auto covariance profile. In particular, $C_Z(\Delta T,\tau_i,\tau_j)$ is proportional to $r_K(\Delta T,\tau_i)$ of Section IVA. Also, the values of ΔT for which $C_Z(\Delta T,\tau_i,\tau_i)$ may be obtained is limited to integral values of the time sampling rate of the channel. In practice, the values obtained for the auto covariance function by the above procedure would be compensated for the effects of additive noise by subtracting out the autocovariance function of the additive noise.

Any of the alternate statistical characterizations of the channel, as well as the gross transmission parameters of the channel, as described in Section IVA may be obtained from the auto covariance profile. In particular, the Fourier transform of the auto covariance profile results in the scattering function characterization of the channel. It should also be noted that before performing the indicated operation in order to obtain the covariance function of the random component it may be possible to smooth or filter the data in order to improve signal to noise ratio as well as to reduce the number of calculations required to determine the auto covariance function. This is possible when the time sampling rate of the channel is much faster than the time variations of the random components of the received signal.

The problem of extracting the mean values of the impulse response, however, cannot always be approached from the point of view of time averaging. Physically, a non zero mean value of the impulse response results from the direct path or any specular path associated with the multipath mechanism. These returns can make the total observed signal nonstationary so that time averaging cannot be performed on the total signal. The particular method of isolating the mean values or specular returns from the random components of the received signal will depend greatly on the characteristics of the particular output. The most frequently used method is to employ some sort of modeling procedure based on an examination of the recorded output. In many cases, for example it may be possible to represent the channel as a combination of one or more specular components containing a number of unknown parameters (i.e., amplitude and doppler frequency) along with a purely random component. The representation of a channel output in terms of one of a set of possible models containing specular as well as purely random components transforms the characterization of the channel into the determination of the unknown parameters as well as the characterization of the random component via its covariance function as has been discussed.

Similar comments also apply to the extraction of the mean values of transfer function, $T_{\omega_0}(t,\Omega)$, from the recorded outputs of the frequency domain measurements. Once the mean value has been determined the process of obtaining the complex time frequency covariance function from the recorded data is adequately given in Reference 11.

V. SUMMARY AND CONCLUSIONS

During the contract period, experimental tests were conducted to measure multipath effects in aircraft-satellite communications links. These tests were performed at 300 MHz between an aircraft flying off the coast of Labrador and the Ohio State University Satellite Facility via the TACSAT satellite relay. The aircraft was supplied and operated by the Avionics Laboratory, Wright-Patterson Air Force Base. In these tests a coded pulsed waveform (6 MHz bandwidth) was generated by the Hazeltine Vericode modem and transmitted by the aircraft. The received signal at O.S.U. was demodulated and recorded using an O.S.U. high speed motion picture camera. The particular reel of film in which the maximum number of consecutive frames of obvious multipath appeared was translated into digital form and onto magnetic tape for further analysis. This transfer consisted of 4096 consecutive frames of motion picture data. The average speed of the camera at which these motion pictures were taken was 103 frames/sec. Thus the time sampling interval was approximately .01 seconds and the duration of digitized data was approximately 40 seconds. This data corresponded to the case where the aircraft was flying in a straight line with elevation angle, altitude and velocity of 4 degrees, 30,000 feet and 400 miles/hour respectively. The differential time delay determined from the digitized data was 3.9 μseconds and the ratio of the power received via the reflected path to the power received via the direct path was -6 dB. No time spreading of the multipath component was detected.

The fluctuation characteristics of the direct and multipath signal amplitudes were analyzed by examining their frequency spectra and auto covariance properties. The results indicate that the direct and multipath fluctuations are very similar in nature and essentially consist of a periodic variation of period approximately 2.5 seconds. It was concluded that this periodic variation was due to the motion of the satellite antenna. Furthermore, there was no evidence of any random components in the multipath amplitude fluctuations that could be attributed to rough surface scattering. From these results, it is concluded that the scattering associated with the multipath transmission at UHF, over the bandwidth of the probing signal, may be characterized as being essentially specular in nature during the time interval corresponding to the processed data.

An analysis was performed to determine the relationship between the physical link parameters of an aircraft satellite communication link and the observable parameters of the communications link. The physical link parameters considered were 1) the directivity of aircraft and satellite antennas, 2) geometry (including motion) of aircraft and satellite and 3) the average reflection coefficient and radar cross section per unit area of the scattering surface associated with the multipath transmission. Numerical results showing the dependence of the differential time delay, differential doppler, power ratio, multipath spread, and fading bandwidth for the above physical link parameters were obtained for two specialized cases. These cases were 1) scattering from a perfectly smooth surface, and 2) scattering from a rough surface. The parameters determined from the multipath flight tests were compared with the calculated results. The results of this comparison tend to support the conclusion that the multipath returns observed during the flight test are primarily specular in nature.

A preliminary investigation was also performed to determine basic experimental techniques which are capable of achieving an adequate characterization of multipath communication channels. In these investigations prime emphasis was put on the determination of modulation and demodulation techniques which are capable of measuring the impulse response function and transfer function, of the transmission channel. Consideration was also given to the data processing required to obtain the mean values and covariance function of the experimentally determined impulse response and transfer function. These latter quantities are required to accurately evaluate the degradation in information transfer due to the transmission channel as well as to determine the choice of modulation and demodulation techniques in order to combat adverse multipath effects.

The basic concepts underlying two specific modulation and demodulation techniques which are theoretically capable of generating a useable functional of the impulse response function have been presented. These were the short pulse and coded pulse waveform (matched

filter) techniques. A frequency domain approach in which a discrete number of c.w. signals are simultaneously transmitted in order to achieve an experimental determination of the transfer function of the channel was also presented.

VI. RECOMMENDATIONS FOR FUTURE WORK

Further study is required to determine basic experimental techniques which can be successfully implemented in order to achieve an adequate characterization of multipath channels. In effect this study would be a continuation of the preliminary experimental design study of Section IV. These investigations would put prime emphasis on the practical implementation of the various techniques discussed in Section IV, i.e., short pulse, matched filter and c.w. approaches in order to determine the impulse response function or transfer function of the transmission channel, as well as on the data processing required to obtain the mean value and covariance function of the experimentally determined impulse response function or transfer function. These latter quantities are required to accurately evaluate the degradation in information transfer due to the transmission channel as well as to determine the choice of modulation and demodulation techniques in order to combat adverse multipath effects.

Specifically, detailed considerations should be given to:

1) The selection of an appropriate probing signal (or signals) (i.e., digital cw or their combination) for a given bandwidth of the transmission channel to be characterized;
2) Modulation and demodulation techniques;
3) Methods of obtaining an adequate signal to noise ratio by means of
   a) signal processing techniques (modems)
   b) antenna gain
   c) transmitter power;
4) Data recording techniques;
5) Data processing techniques.

More multipath measurements at both UHF and L band are also required. A relatively simple and inexpensive method for assessing experimentally communications links at UHF and L band is the short pulse technique. For the actual implementation of the short pulse technique it is recommended that two aircraft be used as the transmitting and receiving sites in order to conduct air to air flight experiments. A characterization of the multipath channel inherent in air to air communication links would not only be of value in itself, but would also serve to characterize multipath channels inherent in aircraft-satellite links due to the similar geometry encountered. Also, in the short pulse air to air configuration a great deal of control over the experiment could be achieved thus providing more reliable data. Furthermore, a large dynamic range (i.e., large

signal to noise ratios) could be obtained in order to determine low level multipath effects.

In the air to air short pulse experiment, short pulses (.1 - .2 μseconds) would be periodically transmitted by the aircraft so that both the direct path and earth's specular point (multipath) will be within the antenna beamwidth. The direct and multipath signals will be received and appropriately demodulated to obtain quadrature components. Single trace photographs of the quadrature components will then be obtained from an oscilloscope display (dual beam scope) using an O.S.U. high speed motion picture camera synchronized with the received signal. In addition, an envelope detector can be inserted prior to the quadrature detection in order to obtain polaroid photographs of the envelope of the received signal. The high speed motion picture film data would be analyzed by computer using the O.S.U. FOSDIC (Film Optical Scanning Device for Computer Input) for translating the photographic records into digital form and onto magnetic tape. The digital data, stored on magnetic tape could then be processed by means of appropriate computer algorithms to obtain the characteristics of the transmission channel, i.e., the mean value and covariance function of the channel impulse response function, which may be directly used in the analysis and design of communication systems.

In order to fully utilize the experimental results obtained from the multipath test series conducted during the current contract period, as well as results from subsequent test series, it is further recommended that theoretical studies be performed to determine modulation and demodulation techniques to combat adverse multipath effects. These studies would put prime emphasis on digital communication systems and would use the channel model determined from the experimental measurements. Theoretical comparisons would be made of several types of modulation and demodulation techniques to determine which gives the best performance.

REFERENCES

1. Richman, D., Page, C.E., and Regis, R., "Study and Experimental Investigation of the Synchronization of Long and Short Range Communications," (U), Hazeltine Research Corporation Report #7687, November 1961. Report Secret

2. Regis, R., Schaefer, L., and Crush, J., "Reliability and Microelectronics Techniques for Anti-Jam Synchronous Circuits," (U), Hazeltine Corporation Technical Report #AFAL-TR-66-160, April 1966. Report Secret.

3. Propagation of Short Radio Waves, Edited by Donald E. Kerr, Boston Technical Publishers, Inc., Massachusetts Institute of Technology Radiation Laboratory Series, 1964, Vol. 13.

4. Peake, W.H., "Theory of Radar Return from Terrain," Report 694-12, 30 April 1959, The Ohio State University ElectroScience Laboratory, Department of Electrical Engineering; prepared under Contract AF 33(616)-3649 for Wright Air Development Center. (AD 216 416)

5. Barrick, D.E., "Rough Surface Scattering Based on the Specular Point Theory," IEEE Transactions on Antennas and Propagation, July 1968.

6. Beckman, P. and Spizzichino, A., The Scattering of Electromagnetic Waves for Rough Surfaces, A Pergamon Press Book, The MacMillan Company, New York, 1963.

7. Durrani, S.H. and Staras, H., "Multipath Problems in Communications between Low-Altitude Spacecraft and Stationary Satellites," RCA Review, Vol. 29, March 1968.

8. Bello, P.A., "Characterization of Randomly Time-Variant Linear Channels," IEEE Trans. on Communications Systems, June 1963.

9. Schwartz, M., Bennett, W. and Stein, S., Communication Systems and Techniques, McGraw-Hill, 1966.

10. Stein, S. and Jones, J.J., Modern Communication Principles, McGraw-Hill, 1967.

11. Bello. P.A., "Measurement of the Complex Time-Frequency Channel Correlation Function," Radio Science, October 1964.

UNCLASSIFIED
Security Classification

DOCUMENT CONTROL DATA - R&D

(Security classification of title, body of abstract and indexing annotation must be entered when the overall report is classified)

1. ORIGINATING ACTIVITY *(Corporate author)*: ElectroScience Laboratroy, Department of Electrical Engineering, The Ohio State University, Columbus, Ohio

2a. REPORT SECURITY CLASSIFICATION: Unclassified

2b. GROUP:

3. REPORT TITLE: MEASUREMENT AND ANALYSIS OF MULTIPATH IN AIRCRAFT-SATELLITE COMMUNICATIONS LINKS AT UHF

4. DESCRIPTIVE NOTES *(Type of report and inclusive dates)*: FINAL TECHNICAL REPORT - 1 November 1968 - 22 March 1971

5. AUTHOR(S) *(Last name, first name, initial)*: Mayhan, John W.

6. REPORT DATE	7a. TOTAL NO. OF PAGES	7b. NO. OF REFS
July 1971	44	11

8a. CONTRACT OR GRANT NO.	9a. ORIGINATOR'S REPORT NUMBER(S)
F 33(615)-69-C-1089 NEW	ElectroScience Laboratory 2734-1
b. PROJECT NO. 4164	
c. TASK	9b. OTHER REPORT NO(S) *(Any other numbers that may be assigned this report)*
d.	AFAL-TR-71-218

10. AVAILABILITY/LIMITATION NOTICES: Distribution limited to U.S. Government agencies only; Test and Evaluation; July 1971. Other requests for this document must be referred to AFAL/AAI, WPAFB Ohio 45433

11. SUPPLEMENTARY NOTES:

12. SPONSORING MILITARY ACTIVITY: Air Force Avionics Laboratory, Air Force Systems Command, Wright-Patterson Air Force Base, Ohio

13. ABSTRACT

This final report summarizes the results of work performed during the period 1 November 1968 to 22 March 1971 under United States Air Force Contract F33615-69-C-1089. A major accomplishment of the work included measurements of multipath in an aircraft-satellite communication link at 300 MHz. Theoretical studies of aircraft-satellite communications links were also performed.

The experimental multipath tests were performed between an aircraft flying off the coast of Labrador and The Ohio State University Satellite Facility via the TACSAT satellite relay. Multipath returns were observed during various portions of the flight tests primarily while the aircraft was in a bank. Polaroid pictures and high speed motion picture data of the received signal were taken throughout the flight tests. The results of reducing 40 seconds of motion picture data (100 frames/second) indicated that the multipath return was essentially specular in nature (i.e., single ray multipath) with an amplitude 6 dB down from the direct signal. The polaroid photographs showed a range of multipath depths ranging from -4 to -9 dB.

DD FORM 1 JAN 64 1473

UNCLASSIFIED
Security Classification

14 KEY WORDS	LINK A		LINK B		LINK C	
	ROLE	WT	ROLE	WT	ROLE	WT
Multipath Channel characterization Aircraft-satellite communications Experimental results						

INSTRUCTIONS

1. ORIGINATING ACTIVITY: Enter the name and address of the contractor, subcontractor, grantee, Department of Defense activity or other organization *(corporate author)* issuing the report.

2*a*. REPORT SECURITY CLASSIFICATION: Enter the overall security classification of the report. Indicate whether "Restricted Data" is included. Marking is to be in accordance with appropriate security regulations.

2*b*. GROUP: Automatic downgrading is specified in DoD Directive 5200.10 and Armed Forces Industrial Manual. Enter the group number. Also, when applicable, show that optional markings have been used for Group 3 and Group 4 as authorized.

3. REPORT TITLE: Enter the complete report title in all capital letters. Titles in all cases should be unclassified. If a meaningful title cannot be selected without classification, show title classification in all capitals in parenthesis immediately following the title.

4. DESCRIPTIVE NOTES: If appropriate, enter the type of report, e.g., interim, progress, summary, annual, or final. Give the inclusive dates when a specific reporting period is covered.

5. AUTHOR(S): Enter the name(s) of author(s) as shown on or in the report. Enter last name, first name, middle initial. If military, show rank and branch of service. The name of the principal author is an absolute minimum requirement.

6. REPORT DATE: Enter the date of the report as day, month, year, or month, year. If more than one date appears on the report, use date of publication.

7*a*. TOTAL NUMBER OF PAGES: The total page count should follow normal pagination procedures, i.e., enter the number of pages containing information.

7*b*. NUMBER OF REFERENCES: Enter the total number of references cited in the report.

8*a*. CONTRACT OR GRANT NUMBER: If appropriate, enter the applicable number of the contract or grant under which the report was written.

8*b*, 8*c*, & 8*d*. PROJECT NUMBER: Enter the appropriate military department identification, such as project number, subproject number, system numbers, task number, etc.

9*a*. ORIGINATOR'S REPORT NUMBER(S): Enter the official report number by which the document will be identified and controlled by the originating activity. This number must be unique to this report.

9*b*. OTHER REPORT NUMBER(S): If the report has been assigned any other report numbers *(either by the originator or by the sponsor)*, also enter this number(s).

10. AVAILABILITY/LIMITATION NOTICES: Enter any limitations on further dissemination of the report, other than those imposed by security classification, using standard statements such as:

(1) "Qualified requesters may obtain copies of this report from DDC."

(2) "Foreign announcement and dissemination of this report by DDC is not authorized."

(3) "U. S. Government agencies may obtain copies of this report directly from DDC. Other qualified DDC users shall request through _____."

(4) "U. S. military agencies may obtain copies of this report directly from DDC. Other qualified users shall request through _____."

(5) "All distribution of this report is controlled. Qualified DDC users shall request through _____."

If the report has been furnished to the Office of Technical Services, Department of Commerce, for sale to the public, indicate this fact and enter the price, if known.

11. SUPPLEMENTARY NOTES: Use for additional explanatory notes.

12. SPONSORING MILITARY ACTIVITY: Enter the name of the departmental project office or laboratory sponsoring *(paying for)* the research and development. Include address.

13. ABSTRACT: Enter an abstract giving a brief and factual summary of the document indicative of the report, even though it may also appear elsewhere in the body of the technical report. If additional space is required, a continuation sheet shall be attached.

It is highly desirable that the abstract of classified reports be unclassified. Each paragraph of the abstract shall end with an indication of the military security classification of the information in the paragraph, represented as *(TS), (S), (C), or (U).*

There is no limitation on the length of the abstract. However, the suggested length is from 150 to 225 words.

14. KEY WORDS: Key words are technically meaningful terms or short phrases that characterize a report and may be used as index entries for cataloging the report. Key words must be selected so that no security classification is required. Identifiers, such as equipment model designation, trade name, military project code name, geographic location, may be used as key words but will be followed by an indication of technical context. The assignment of links, rules, and weights is optional.